Preprint typeset in JHEP style - HYPER VERSION 2015

arXiv:1601.05864v1 [hep-th] 22 Jan 2016

CHY-construction of Planar Loop Integrands of Cubic Scalar Theory

Bo Feng[1,2]

[1] *Zhejiang Institute of Modern Physics*
Physics Department, Zhejiang University
PR China, 310027

[2] *Niels Bohr International Academy and Discovery Center*
The Niels Bohr Institute, University of Copenhagen,
Blegdamsvej 17, DK-2100 Copenhagen, Denmark

Abstract: In this paper, by treating massive loop momenta to massless momenta in higher dimension, we are able to treat all-loop scattering equations as tree ones. As an application of the new aspect, we consider the CHY-construction of bi-adjoint ϕ^3 theory. We present the explicit formula for two-loop planar integrands. We discuss carefully how to subtract various forward singularities in the construction. We count the number of terms obtained by our formula and by direct Feynman diagram calculation and find the perfect match, thus provide a strong support for our results.

Keywords: Scattering Equation, Two-loop Integrand, Dimensional Deformation.

Contents

1. Introduction **1**

2. Tree-level amplitude of color ordered bi-adjoint ϕ^3 theory **3**

3. All Loop scattering equations **8**

4. Two-loop CHY-integrand of ϕ^3 theory **13**

4.1 Analysis of two-loop Feynman diagrams 13

4.2 Special Feynman diagrams 16

4.3 The construction of CHY-integrand 19

4.3.1 The CHY-integrand for ordering $\mathcal{O}_{jk}$ 20

4.3.2 The CHY-integrand for ordering $\mathcal{O}_j$ 24

4.4 The CHY-construction of reducible two-loop diagrams 26

5. Counting **28**

5.1 Counting from CHY-formula 29

5.2 Counting from Feynman diagrams 30

6. Conclusion **31**

1. Introduction

The discovery of CHY-formula for tree-level scattering amplitudes by Cachazo, He and Yuan [CHY] in a series of papers [1, 2, 3, 4, 5] has provided a novel way to calculate and understand scattering amplitudes. In this construction, a set of algebraic equations (called the **scattering equations**) has played a crucial role. These equations appear in the literature in a variety of contexts [6, 7, 8, 9, 10, 11, 12, 13, 14]. More explicitly, scattering equations of n-particles are given by

$$\mathcal{S}_a \equiv \sum_{b\neq a} \frac{2k_a \cdot k_b}{z_{ab}}, \qquad z_{ab} \equiv z_a - z_b, \qquad a = 1, 2, ..., n \ , \tag{1.1}$$

where the z_a is the location of a-th particle in the Riemann surface. Although there are n equations, only $(n-3)$ of them are independent, which can be seen by following three identities among them:

$$\sum_a \mathcal{S}_a = 0, \qquad \sum_a \mathcal{S}_a z_a = 0, \qquad \sum_a \mathcal{S}_a z_a^2 = 0, \tag{1.2}$$

under the momentum conservation and null conditions $k_a^2 = 0$. The tree-level amplitude is calculated by following formula

$$\mathcal{A}_n = \int \frac{(\prod_{a=1}^n dz_a)}{d\omega} \Omega(\mathcal{S}) \mathcal{I}, \qquad d\omega = \frac{dz_r dz_s dz_t}{z_{rs} z_{st} z_{tr}} \tag{1.3}$$

where $\mathcal{I}$ is the so called **CHY-integrand** and $d\omega$ is the volume of $SL(2, C)$ group, where we have used the symmetry to fix locations of three variables z_r, z_s, z_t. The $\Omega(\mathcal{S})$ is given by

$$\Omega(\mathcal{S})_{ijm} = z_{ij} z_{jm} z_{mi} \prod_{a \neq i,j,k,m} \delta\left(\mathcal{S}_a\right) \tag{1.4}$$

where $(n-3)$-independent delta-functions of scattering equations have been imposed. Since there are $(n-3)$ variables and $(n-3)$ equations, there is no integration left to do in (1.3). For each solution of delta-functions, we get a result after inserting it into the CHY-integrand $\mathcal{I}$. The amplitude is given by summing over all $(n-3)!$ results.

The correctness of CHY-formula has been understood from various points of view. In [15], using the BCFW on-shell recursion relation [16, 17] the validity of the CHY construction for ϕ^3 theory and Yang-Mills theory has been proved. Using ambitwistor string theory [18, 19, 20, 21, 22, 23, 24, 25, 27, 26, 28], by calculating corresponding correlation functions of different world-sheet fields, different CHY-formulas for different theories have been derived alongside with the natural appearance of scattering equations. In [29], inspired by the field theory limit of string theory, a dual model has been introduced. Using this idea, a direct connection between the CHY-formula and the standard tree-level Feynman diagrams has been established in [30, 31].

The CHY-formula (or CHY-construction) has divided calculating scattering amplitudes of a given theory into two parts: (a) finding solutions of scattering equations and (b) finding the corresponding CHY-integrand $\mathcal{I}$, which is the rational functions of locations z_a for the given theory. Among these two parts, the former task is universal for all theories while the later task does depend on the detail of theories. Although there are some general principles to guide the construction of CHY-integrands, we still do not know the general algorithm for all theories. However, amazing progress has been made in [5] where integrands are known for many theories.

Although looks simple, scattering equations are not so easy to solve. By proper transformation, scattering equations become a set of algebraic equations as shown in [33]. From this aspect, several work has appeared [34, 35, 36, 37, 38, 39] by exploring the powerful computational algebraic geometry method, such as the companion matrix, the Bezoutian matrix, the elimination theorem. A different approach is given in [40] by mapping the problem to the known result of bi-adjoint ϕ^3 theory. Using the generalized KLT relation and Hamiltonian decompositions of certain 4-regular graphs, one can bypass solving scattering equations and read out results directly. Another powerful method is given in [30, 31], where a mapping rule between CHY-integrands and tree-level Feynman diagrams has been given. In this paper, we will use the mapping rule heavily and related results have been given in the Appendix A.

Encouraged by the success at tree-level, a lot of efforts have been done to generalize to loop-level [21, 24, 25]. A breakthrough is given in [28] by Geyer, Mason, Monteiro and Tourkine [28]. They show how to reduce the problem of genus one to a modified problem on the Riemann sphere, where the analysis is essentially as at tree-level. Using the picture, they provide a conjecture to any loop order. In [41, 42], the one-loop integrand of bi-adjoint ϕ^3 theory has been proposed, while in [43, 44] more general theories such as Yang-Mills theory and gravity theory have been treated at the one-loop level. Among these results, the generalization of mapping rule to one-loop level given in [41] will be very useful. In fact, in this paper, we will show that this mapping rule could be generalized to all loops.

In this paper, we will generalize above one-loop results to higher loops. We will write down all loop scattering equations. The key idea of our approach is to treat massive loop momenta as massless momenta in a higher dimension. Using the idea, we effectively reduce the loop problem to tree one. In fact, the same idea has been explored by the $\mathcal{Q}$-cut construction in [45, 46]. After having loop scattering equations, we construct the CHY-integrand, which will produce two-loop planar integrand of bi-adjoint ϕ^3 theory.

The plan of the paper is following. In the section two, we have reviewed the mapping rule between CHY-integrands and Feynman diagrams of bi-adjoint ϕ^3 theory and discussed how to write down CHY-integrands for tree diagrams with a given set of poles. In the section three, we discuss all loop scattering equations. In the section four, we construct the two-loop CHY-integrand for ϕ^3 theory. To carry out the construction, we have carefully discussed related forward singularities when sewing tree to become loops and how to remove them. In the section five, by the matching of the number of terms obtained by CHY-construction and by Feynman diagrams, we provide a strong support for our result. In the section six, a brief conclusion is given.

2. Tree-level amplitude of color ordered bi-adjoint ϕ^3 theory

In this part, we will review relevant results of color ordered bi-adjoint ϕ^3 theory at tree-level, especially the mapping rule between tree-level Feynman diagrams and tree-level CHY-integrands. Using this mapping rule, we can discuss how to remove certain Feynman diagrams from a given CHY-integrand. Before doing so, let us define following compact notation

$$[i_1, i_2, \ldots, i_m] \equiv \sum_{1\leq a<b\leq m} 2k_{i_a}\cdot k_{i_b}\ . \tag{2.1}$$

Now we discuss the mapping rule given in [30, 31]. First it is worth to notice that by Mobius invariance each factor z_i should have degree -4 in the CHY-integrand, thus one can represent the CHY-integrand by a graph, where each factor $z_{ij}\equiv(z_i-z_j)$ in the denominator corresponds to one (arrowed) solid line connecting vertexes i,j and each factor z_{ij} in the numerator corresponds to one (arrowed) dash line connecting vertexes i,j. Such graph will be called the CHY-graph. Given a CHY-integrand (or CHY-graph), the result obtained from CHY-formula will a sum of inverse-products of multi-index Mandelstam

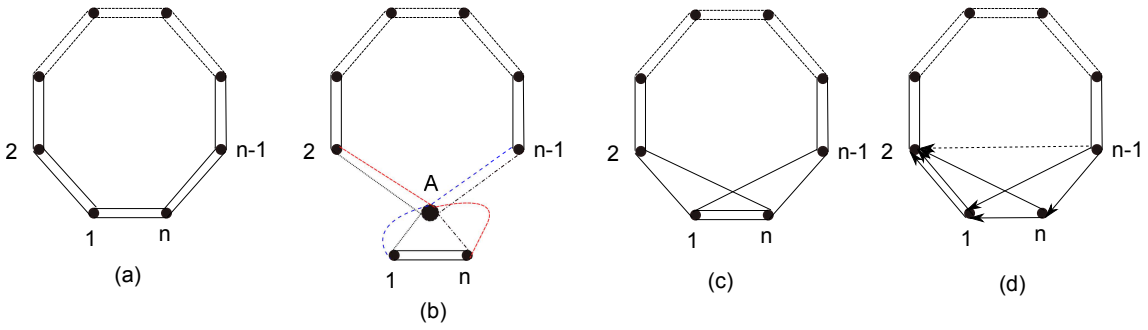

Figure 1: The CHY-graph for Feynman diagrams with pole s_{n1}. (a) The CHY-graph for full n-point tree-level amplitude; (b) The "pinching" picture where the new vertex A represents the combination of vertexes $1, n$. (c) The CHY-graph for Feynman diagrams containing pole s_{n1} obtained from (b) after lifting the $(n-1)$-point graph to the n-point graph. (d) The CHY-graph after subtracting (c) from (a), where we have used arrows to indicate the direction.

invariants denoted $s_{i_1\ldots i_m} = (k_{i_1} + \ldots + k_{i_m})^2 = [i_1, i_2, \ldots, i_m]$ when all $k_i^2 = 0$, i.e.,

$$\prod_{a=1}^{n-3} 1/s_{P_a} = \prod_{a=1}^{n-3} \frac{1}{[P_a]}, \tag{2.2}$$

for n-point tree-level amplitudes. Each $P_a \subset \{1, \ldots, n\}$ denotes a subset of legs that we can always take to have at most $n/2$ elements (because $s_P = s_{P^{\complement}}$, with $P^{\complement} \equiv \mathbb{Z}_n \backslash P$, by momentum conservation). The collections of subsets $\{P_a\}$ appearing in (2.2) must satisfy the following criteria:

- for each pair of indices $\{i, j\} \subset P_a$ in each subset P_a, there are exactly $(2|P_a| - 2)$ factors of $(z_i - z_j)$ appearing in the denominator of $\mathcal{I}(z_1, \ldots, z_n)$;
- each pair of subsets $\{P_a, P_b\}$ in the collection is either nested or complementary—that is, $P_a \subset P_b$ or $P_b \subset P_a$ or $P_a \subset P_b^{\complement}$ or $P_b^{\complement} \subset P_a$;

If there are no collections of $(n-3)$ subsets $\{P_a\}$ satisfying the criteria above, the result of integration will be zero. One simple example using above rule is that

$$\frac{1}{z_{12}^2 z_{23} z_{34} z_{45} z_{15} z_{35}^2 z_{14} z_{24}} \Longleftrightarrow \frac{1}{s_{12} s_{35}} \tag{2.3}$$

Another important example is the CHY-integrand for the full tree-level amplitude of ϕ^3 theory with ordering $\{1, 2, ..., n\}$ (the corresponding CHY-graph is given by the diagram (a) in the Figure 1)

$$\mathcal{I}_n^{CHY}(\{1, 2, ..., n\}) = \frac{1}{z_{12}^2 z_{23}^2 \ldots z_{(n-1)n}^2 z_{n1}^2} \ . \tag{2.4}$$

There is one fundamental formula, which will be useful later: the number of color ordered n-point tree-level Feynman diagrams of ϕ^3 theory is given by

$$C(n) = \frac{2^{n-2}(2n-5)!!}{(n-1)!} \ . \tag{2.5}$$

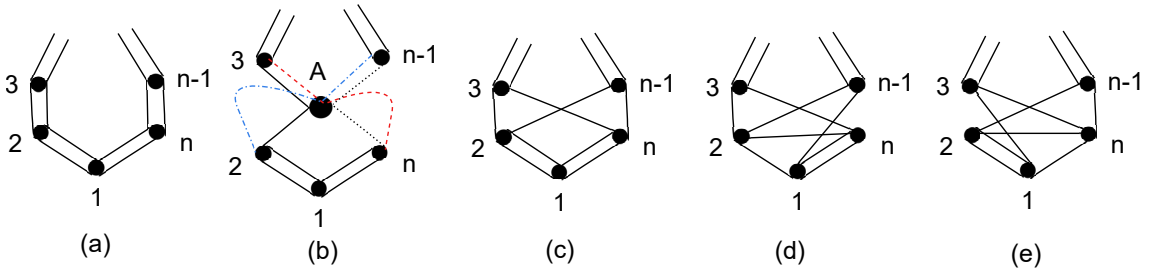

Figure 2: (a) The CHY-graph for full n-point tree-level amplitude; (b) The "pinching" picture where the new vertex A represents the combination of vertexes $n, 1, 2$. (c) The CHY-graph for all Feynman diagrams with pole s_{n12} obtained from (b) after lifting the $(n-2)$-point graph to the n-point graph. (d) The CHY-graph having the fixed poles s_{n12} and s_{n1}; (e) The CHY-graph having the fixed poles s_{n12} and s_{12};

Having presented the rule above, we try to find the CHY-integrand which gives Feynman diagrams of certain type, such as these in the Figure 3 and the Figure 8. Let us start with the simplest case, i.e., the (B-2) type of Figure 3, where we assume that $1, n$ are always attached to the same cubic vertex and then they combine together to connect to other legs. If we cut the propagator s_{1n}, we will be left with color ordered full tree-level amplitude with $(n-1)$-legs. This picture motivates us an operation called the "**pinching**" where vertexes $1, n$ are combined to become a new vertex A (see the diagram (b) in the Figure 1). It is worth to notice that in (b) we have drawn four lines in different colors and styles to emphasize when we lift the $(n-1)$-point graph to n-point graph, how these lines are connected. Also the group $A, 1, 2$ itself is the CHY-graph corresponding to the expression (2.4) with $n = 3$. The lift graph of (b) is given in the diagram (c) in the Figure 1. When translating above manipulation at the graph level to expression, we find that

$$\mathcal{I}^{CHY}_{n;s_{n1}}(\{1,2,...,n\}) = \frac{1}{z^2_{23}...z^2_{(n-2)(n-1)}\left(z_{(n-1)n}z_{(n-1)1}\left(z^2_{n1}\right)z_{n2}z_{12}\right)} \tag{2.6}$$

Using the mapping rule, one can check that the CHY-integrand (2.6) will give expression contains $C(n-1)$ terms with the fixed pole s_{n1} (see Eq.(2.5)), which is the right counting number. Now it is obvious that if we want to remove these Feynman diagrams of the (B-2) type, we should subtract the CHY-integrand (2.6) from the CHY-integrand (2.4) and get

$$\begin{aligned}&\frac{1}{z^2_{23}...z^2_{(n-2)(n-1)}}\left\{\frac{1}{z^2_{(n-1)n}z^2_{n1}z^2_{12}}-\frac{1}{z_{(n-1)n}z_{(n-1)1}z^2_{n1}z_{n2}z_{12}}\right\}\\ =&\frac{1}{z^2_{23}...z^2_{(n-2)(n-1)}}\frac{z_{(n-1)2}}{z^2_{(n-1)n}z_{(n-1)1}z_{n1}z_{n2}z^2_{12}}\end{aligned} \tag{2.7}$$

where the explicit pole z^2_{n1} in the denominator has been canceled. The final CHY-integrand can be represented by the diagram (d) in the Figure 1.

Having done the simplest case, now we consider the CHY-integrand, which produces all Feynman diagrams containing a given pole, for example, s_{n12}. Again we can pinch three vertexes $n, 1, 2$ together to reduce n-legs to $(n-2)$-legs (see the diagram (b) in Figure 2). After lifting we get the CHY-graph (see the diagram (c) in Figure 2), which contains all Feynman diagrams having the pole s_{n12}. The corresponding CHY-integrand is obtained by replacing $z_{(n-1)n}^2\left(z_{n1}^2 z_{12}^2\right) z_{23}^2$ in the denominator of (2.4) to the factor $z_{(n-1)n}z_{(n-1)2}\left(z_{n1}^2 z_{12}^2\right) z_{n3}z_{23}$, i.e.,

$$\mathcal{I}_{n;s_{n12}}^{CHY}(\{1,2,...,n\}) = \frac{1}{z_{34}^2...z_{(n-2)(n-1)^2}\left(z_{(n-1)n}z_{(n-1)2}\left(z_{n1}^2 z_{12}^2\right) z_{n3}z_{23}\right)} \tag{2.8}$$

If we subtract the CHY-integrand (2.8) from the CHY-integrand (2.4), we will get

$$\begin{aligned}&\frac{1}{z_{34}^2...z_{(n-2)(n-1)}^2}\left\{\frac{1}{z_{(n-1)n}^2\left(z_{n1}^2 z_{12}^2\right) z_{23}^2} - \frac{1}{z_{(n-1)n}z_{(n-1)2}\left(z_{n1}^2 z_{12}^2\right) z_{n3}z_{23}}\right\}\\ &= \frac{1}{z_{34}^2...z_{(n-2)(n-1)}^2}\frac{z_{(n-1)3}z_{n2}}{z_{(n-1)n}^2 z_{(n-1)2}\left(z_{n1}^2 z_{12}^2\right) z_{n3}z_{23}^2}\ .\end{aligned} \tag{2.9}$$

Using the "pinching" operation above pattern can be easily generalized to find the CHY-integrand which produces all Feynman diagrams containing a given pole, for example, $s_{n12..k}$. What we need to do is following replacement of the factor $z_{(n-1)n}^2\left(z_{n1}^2 z_{12}^2...z_{(k-1)k}^2\right) z_{k(k+1)}^2$ in the denominator of (2.4) to the factor $z_{(n-1)n}z_{(n-1)k}\left(z_{n1}^2 z_{12}^2...z_{(k-1)k}^2\right) z_{n(k+1)}z_{k(k+1)}$, i.e.,

$$\frac{1}{...z_{(n-1)n}^2\left(z_{n1}^2 z_{12}^2...z_{(k-1)k}^2\right) z_{k(k+1)}^2...} \Longrightarrow \frac{1}{...z_{(n-1)n}z_{(n-1)k}\left(z_{n1}^2 z_{12}^2...z_{(k-1)k}^2\right) z_{n(k+1)}z_{k(k+1)}...}\ . \tag{2.10}$$

Above replacement rule can be nicely represented as following: *for each fixed pole $s_{n12..k}$ we multiply by a corresponding factor*

$$\mathcal{P}[n-1,n,k,k+1] \equiv \frac{z_{(n-1)n}z_{k(k+1)}}{z_{(n-1)k}z_{n(k+1)}} \tag{2.11}$$

where n, k as the first and the last legs in the ordering of the specified pole.

Having observed the pattern, now it is easy to write down the corresponding CHY-integrand with a given pole structure (we will call it as the "signature"). Let us give a few examples:

- With fixed poles s_{n12} and s_{456}, the integrand is given by $\mathcal{I}_n^{CHY}(\{1,2,...,n\})\mathcal{P}[n-1,n,2,3]\mathcal{P}[3,4,6,7]$.
- With fixed poles s_{12} and s_{34}, the integrand is given by $\mathcal{I}_n^{CHY}(\{1,2,...,n\})\mathcal{P}[n,1,2,3]\mathcal{P}[2,3,4,5]$. It is worth to notice that z_{23}^2 in numerator will cancel the z_{23}^2 in denominator of $\mathcal{I}_n^{CHY}$.
- With fixed poles s_{n1} and s_{n12}, the integrand is given by $\mathcal{I}_n^{CHY}(\{1,2,...,n\})\mathcal{P}[n-1,n,1,2]\mathcal{P}[n-1,n,2,3]$. For this case, pole s_{n1} is inside the pole s_{n12}.

Above examples have only two poles and it is easy to check that the numerator of the final expression is one. Thus we can check our claim easily using the mapping rule (2.2). However, when we fix three or more poles, some interesting thing happens: the numerator of final expression could be nontrivial. For example, with the signature $s_{12}s_{123}s_{1234}$ at eight points, after applying our rule (2.11) we get

$$\frac{z_{81}}{z_{12}^2 z_{23} z_{34} z_{45} z_{56}^2 z_{67}^2 z_{78}^2 z_{84} z_{15} z_{83} z_{14} z_{82} z_{13}} \ . \tag{2.12}$$

Since the numerator is not one, we could not apply the mapping rule directly. To solve the problem, we need to use following identity

$$\frac{z_{ab} z_{dc}}{z_{ac} z_{bc}} = \frac{z_{ad}}{z_{ac}} - \frac{z_{bd}}{z_{bc}} \ . \tag{2.13}$$

Applying to our case with $z_{ab} = z_{81}$, we need to find c, d. There are some conditions. First the degree of factor z_{dc} in the denominator of original expression can only be zero or one. Thus, after multiplying $1 = \frac{z_{dc}}{z_{dc}}$ and then applying identity (2.13), we will not end up with factor z_{dc} having degree more than two in denominator. Secondly, we should require the original expression has factors z_{ac}, z_{bc} in denominator to give the left handed side of (2.13). Finally, we should require the original expression has factors z_{ad} and z_{bd} in denominator to cancel the corresponding factor in numerator appearing after using (2.13). If we can find such d, c, we can reduce the problem to trivial one and then apply our mapping rule. For the example given in (2.12), it is easy to see that d, c can be chosen from $\{2, 3, 4\}$. In fact, there are six possible choices and we have checked each one. With the choice $c = 2, d = 3$ we have

$$\begin{aligned}
&\frac{z_{81}}{z_{12}^2 z_{23} z_{34} z_{45} z_{56}^2 z_{67}^2 z_{78}^2 z_{84} z_{15} z_{83} z_{14} z_{82} z_{13}} = \frac{-1}{z_{12} z_{23}^2 z_{34} z_{45} z_{56}^2 z_{67}^2 z_{78}^2 z_{84} z_{15} z_{83} z_{14} z_{13}} \times \frac{z_{81} z_{32}}{z_{82} z_{12}} \\
&= \frac{-1}{z_{12} z_{23}^2 z_{34} z_{45} z_{56}^2 z_{67}^2 z_{78}^2 z_{84} z_{15} z_{83} z_{14} z_{13}} \left(\frac{z_{83}}{z_{82}} - \frac{z_{13}}{z_{12}} \right) \\
&= \frac{-1}{z_{12} z_{23}^2 z_{34} z_{45} z_{56}^2 z_{67}^2 z_{78}^2 z_{84} z_{15} z_{82} z_{14} z_{13}} + \frac{+1}{z_{12}^2 z_{23}^2 z_{34} z_{45} z_{56}^2 z_{67}^2 z_{78}^2 z_{84} z_{15} z_{83} z_{14}} \ .
\end{aligned} \tag{2.14}$$

Using the mapping rule, we can calculate each term and sum them up. It is easy to check that they indeed give all terms having above signature.

We can continue to more complicated examples, for example, the one with signature $s_{12}s_{123}s_{1234}s_{12345}$ at eight points. One more pole means to multiply another factor

$$\begin{aligned}
&\frac{z_{81}}{z_{12}^2 z_{23} z_{34} z_{45} z_{56}^2 z_{67}^2 z_{78}^2 z_{84} z_{15} z_{83} z_{14} z_{82} z_{13}} \times \frac{z_{81} z_{56}}{z_{85} z_{16}} \\
&= \left(\frac{-1}{z_{12} z_{23}^2 z_{34} z_{45} z_{56}^2 z_{67}^2 z_{78}^2 z_{84} z_{15} z_{82} z_{14} z_{13}} + \frac{+1}{z_{12}^2 z_{23}^2 z_{34} z_{45} z_{56}^2 z_{67}^2 z_{78}^2 z_{84} z_{15} z_{83} z_{14}} \right) \times \frac{z_{81} z_{56}}{z_{85} z_{16}}
\end{aligned} \tag{2.15}$$

where we have used the result (2.14). Now we use similar idea to do decomposition of these two terms. For the first term we take $c = 2, d = 4$ and obtain

$$\frac{-1}{z_{23}^2 z_{34} z_{45} z_{56} z_{67}^2 z_{78}^2 z_{82} z_{15} z_{14} z_{13} z_{85} z_{16} z_{42}} + \frac{+1}{z_{23}^2 z_{34} z_{45} z_{56} z_{67}^2 z_{78}^2 z_{84} z_{15} z_{12} z_{13} z_{85} z_{16} z_{42}} \ . \tag{2.16}$$

For the second term, we take $c = 5, d = 4$ and get

$$\frac{1}{z_{12}^2 z_{23}^2 z_{34} z_{45}^2 z_{56} z_{67}^2 z_{78}^2 z_{85} z_{83} z_{14} z_{16}} + \frac{-1}{z_{12}^2 z_{23}^2 z_{34} z_{45}^2 z_{56} z_{67}^2 z_{78}^2 z_{84} z_{83} z_{15} z_{16}} \ . \tag{2.17}$$

Using the mapping rule to above four terms and summing them up, we do get all terms having the signature of four fixed poles.

3. All Loop scattering equations

In this section, we will discuss general m-th loop scattering equations. First we will review the construction given in [28], then we give another understanding of these equations from the point view of higher dimension. To establish the relation between m-th loop n-point scattering equations and tree scattering equations of $(n + 2m)$-points, we use following convention: k_i, $i = 1, ..., n$ for momenta of n external legs, while $k_{n+2j-1} = -k_{n+2j}$ with $j = 1, ..., m$ for the j-th loop momentum. While we still impose $k_i^2 = 0$ for $i = 1, ..., n$, loop momenta k_{n+2j-1} are general massive.

To derive loop scattering equations, we start from the m-th loop one-form

$$P = \sum_{r=1}^{m} k_{n+2r-1} \frac{(z_{n+2r-1} - z_{n+2r})dz}{(z - z_{n+2r-1})(z - z_{n+2r})} + \sum_{i=1}^{n} k_i \frac{dz}{z - z_i} \tag{3.1}$$

where $z_i, i = 1, .., n$ are marked points for external legs while z_{n+2r-1}, z_{n+2r}, $r = 1, ..., m$ are new marked points for pinching Riemann sphere. It is easy to see that P^2 contains double poles, thus we define

$$S(z) = P^2 - \sum_{r=1}^{m} k_{n+2r-1}^2 \frac{(z_{n+2r-1} - z_{n+2r})^2 d^2 z}{(z - z_{n+2r-1})^2 (z - z_{n+2r})^2} \ , \tag{3.2}$$

which contains only single poles at all marked points z_i, $i = 1, 2..., n + 2m$. Calculating these residues, we get

$$\mathcal{S}_a = \sum_{j \neq a,1}^{n} \frac{2k_a \cdot k_j}{z_a - z_j} + \sum_{t=1}^{m} \left(\frac{2k_a \cdot k_{n+2t-1}}{z_a - z_{n+2t-1}} + \frac{2k_a \cdot k_{n+2t}}{z_a - z_{n+2t}} \right), \quad 1 \leq a \leq n \tag{3.3}$$

for n external marked points and

$$\begin{aligned} \mathcal{S}_{n+2t-1} &= \sum_{a=1}^{n} \frac{2k_{n+2t-1} \cdot k_a}{z_{n+2t-1} - z_a} + \sum_{s=1, s \neq t}^{m} \left(\frac{2k_{n+2t-1} \cdot k_{n+2s-1}}{z_{n+2t-1} - z_{n+2s-1}} + \frac{2k_{n+2t-1} \cdot k_{n+2s}}{z_{n+2t-1} - z_{n+2s}} \right) \ , \\ \mathcal{S}_{n+2t} &= \sum_{a=1}^{n} \frac{2k_{n+2t} \cdot k_a}{z_{n+2t} - z_a} + \sum_{s=1, s \neq t}^{m} \left(\frac{2k_{n+2t} \cdot k_{n+2s-1}}{z_{n+2t} - z_{n+2s-1}} + \frac{2k_{n+2t} \cdot k_{n+2s}}{z_{n+2t} - z_{n+2s}} \right), \quad 1 \leq t \leq m \end{aligned} \tag{3.4}$$

for new marked points corresponding to the t-th loop momentum. These $(n + 2m)$ equations given in (3.3) and (3.4) are the m-th loop scattering equations we are looking for.

Now we compare these equations with the corresponding tree-level scattering equations of $(n+2m)$-points given by

$$\mathcal{S}_a \equiv \sum_{b\neq a} \frac{2k_a\cdot k_b}{z_a - z_b}, \qquad a = 1, 2, ..., n+2m. \tag{3.5}$$

They are exactly same for $a = 1, ..., n$, except the remaining $2m$ momenta satisfying $k_{n+2j-1} = -k_{n+2j}$ (i.e., in the forward limit). However, for $a = n+1, ..., n+2m$, terms like $\frac{2k_{n+2t-1}\cdot k_{n+2t}}{z_{n+2t-1}-z_{n+2t}}$ in tree-level scattering equations have been dropped in the m-th loop scattering equations. The dropping of these terms can, in fact, be traced back to the numerator $(z_{n+2r-1} - z_{n+2r})$ of the first term in (3.1). This difference is crucial as we will explain later.

Having obtained loop scattering equations, let us check their Mobius covariance. Under the Mobius transformation $z' = \frac{az+b}{cz+d}$, one find

$$z'_{ij} = \frac{(ad-bc)}{(cz_i+d)(cz_j+d)} z_{ij} \ , \tag{3.6}$$

thus it is easy to check that for $\mathcal{S}_{1\leq a\leq n}$ we have

$$\begin{aligned}
\mathcal{S}_a \to & \frac{(cz_a+d)}{(ad-bc)}\left\{\sum_{j\neq a,1}^{n}\frac{2k_a\cdot k_j(cz_j+d)}{z_a-z_j} + \sum_{t=1}^{m}\left(\frac{2k_a\cdot k_{n+2t-1}(cz_{n+2t-1}+d)}{z_a-z_{n+2t-1}} + \frac{2k_a\cdot k_{n+2t}(cz_{n+2t}+d)}{z_a-z_{n+2t}}\right)\right\} \\
= & \frac{(cz_a+d)}{(ad-bc)}\left\{\sum_{j\neq a,1}^{n}\left(\frac{2k_a\cdot k_j(cz_a+d)}{z_a-z_j} - 2k_a\cdot k_j\right)\right. \\
& \left. + \sum_{t=1}^{m}\left(\frac{2k_a\cdot k_{n+2t-1}(cz_a+d)}{z_a-z_{n+2t-1}} - 2k_a\cdot k_{n+2t-1} + \frac{2k_a\cdot k_{n+2t}(cz_a+d)}{z_a-z_{n+2t}} - 2k_a\cdot k_{n+2t}\right)\right\} \\
= & \frac{(cz_a+d)^2}{(ad-bc)}\mathcal{S}_a \ ,
\end{aligned} \tag{3.7}$$

and for $\mathcal{S}_{n<a\leq n+2m}$ we have

$$\begin{aligned}
\mathcal{S}_{n+2t-1} \to & \frac{(cz_{n+2t-1}+d)}{(ad-bc)}\left\{\sum_{a=1}^{n}\frac{2k_{n+2t-1}\cdot k_a(cz_a+d)}{z_{n+2t-1}-z_a}\right. \\
& \left.+\sum_{s=1,s\neq t}^{m}\left(\frac{2k_{n+2t-1}\cdot k_{n+2s-1}(cz_{n+2s-1}+d)}{z_{n+2t-1}-z_{n+2s-1}}+\frac{2k_{n+2t-1}\cdot k_{n+2s}(cz_{n+2s}+d)}{z_{n+2t-1}-z_{n+2s}}\right)\right\} \\
= & \frac{(cz_{n+2t-1}+d)}{(ad-bc)}\left\{\sum_{a=1}^{n}\left(\frac{2k_{n+2t-1}\cdot k_a(cz_{n+2t-1}+d)}{z_{n+2t-1}-z_a}-2k_{n+2t-1}\cdot k_a\right)\right. \\
& +\sum_{s=1,s\neq t}^{m}\left(\frac{2k_{n+2t-1}\cdot k_{n+2s-1}(cz_{n+2t-1}+d)}{z_{n+2t-1}-z_{n+2s-1}}-2k_{n+2t-1}\cdot k_{n+2s-1}\right. \\
& \left.\left.+\frac{2k_{n+2t-1}\cdot k_{n+2s}(cz_{n+2t-1}+d)}{z_{n+2t-1}-z_{n+2s}}-2k_{n+2t-1}\cdot k_{n+2s}\right)\right\} \\
= & \frac{(cz_{n+2t-1}+d)^2}{(ad-bc)}\mathcal{S}_{n+2t-1}
\end{aligned} \tag{3.8}$$

with similar expressions for $\mathcal{S}_{n+2t}$.

The covariance indicates that there are three relations among these $(n+2m)$ scattering equations:

$$\sum_{i=1}^{n+2m}\mathcal{S}_i=0,\qquad \sum_{i=1}^{n+2m}z_i\mathcal{S}_i=0,\qquad \sum_{i=1}^{n+2m}z_i^2\mathcal{S}_i=0\ . \tag{3.9}$$

We want to emphasize that in above calculations, we have used only following three conditions: (1) massless condition $k_i^2=0$ for $i=1,...,n$; (2) momentum conservation $\sum_{i=1}^{n}k_i=0$; (3) forward limit $k_{n+2j-1}=-k_{n+2j}$ for $j=1,...,m$. In other words, we do not need to impose $k_{n+2j-1}^2=0$, which is one consequence of dropped terms like $\frac{2k_{n+2t-1}\cdot k_{n+2t}}{z_{n+2t-1}-z_{n+2t}}$. In fact, it can be easily checked that without dropping these terms, the second and third relation in (3.9) can not be satisfied with above three conditions.

Now let us try to understand the meaning of dropping terms like $\frac{2k_{n+2t-1}\cdot k_{n+2t}}{z_{n+2t-1}-z_{n+2t}}$. It is obviously that if $k_{n+2t-1}\cdot k_{n+2t}=-k_{n+2t}^2=0$, it will disappear automatically. However, since they are loop momenta we should not expect these conditions. To make these two aspects consistent to each other, one nice idea is to use the *dimension reduction*. Let us assume that all external momenta are in D-dimensional spacetime, then we can treat massive momenta in the D-dimensional spacetime to be massless momenta in $(D+d)$-dimensional spacetime. This can be arranged because scattering equations are dimensional blind. In fact, using the idea, several groups have noticed that scattering equations for massive particles[1] at tree-level first proposed by Naculich in [47] can be understood from this point of view. More explicit, let us rewrite the $(D+d)$-dimensional scattering equations as

$$\sum_{j\neq i}\frac{\widetilde{k}_i\cdot\widetilde{k}_j}{z_i-z_j}=\sum_{j\neq i}\frac{k_i\cdot k_j+\Delta_{ij}}{z_i-z_j} \tag{3.10}$$

[1]Other related works for massive particles can be found in [15, 48, 49, 50]

where each $(D+d)$-dimensional momentum $\widetilde{k} = k + \eta$ has been split into momentum k in D-dimension and momentum η in d-dimension, so $\Delta_{ij} = -\eta_i \cdot \eta_j$. It is easy to see that $\Delta_{ij} = \Delta_{ji}$ and $\sum_{j\neq i} \Delta_{ij} = \eta_i \cdot \eta_i$ by momentum conservation in d-dimension. Thus massless condition $k_i^2 - \eta_i^2 = 0$ in $(D+d)$-dimension gives the mass $\sum_{j\neq i} \Delta_{ij} = m_i^2$ in D-dimension.

Above discussions lead us to a new understanding of these m-th loop scattering equations in D-dimension: *they are the tree-level scattering equations of $(n+2m)$-points under the forward limit, where $2m$'s momenta are massless in $(D+d)$-dimension while n external momenta are massless in D-dimension.* An immediate implication is that all contractions of the type $2k_{n+2t-1}\cdot k_{n+2s-1}$ in (3.4) should be understood as the contractions in $(D+d)$-dimension.

The new understanding of loop momenta in higher dimension has led an important application: since from the point of view of higher dimension they are massless, we have effectively cut m's internal lines, so m-th loop Feynman diagrams open up to become connected tree-level Feynman diagrams. This idea has been used in [41] to construct one-loop CHY integrands of ϕ^3 theory (see also [42, 43, 44]). A more intensive application of reducing loop problems to tree-level ones has been demonstrated in the $\mathcal{Q}$-cut construction [45] (see also [46]). In this paper, we will use the same idea to write down CHY loop integrands from corresponding tree ones.

Having understood the similarity and the connection with tree-level cases, it is natural to write down the integration formula for loop amplitudes as proposed in [28]

$$\mathcal{A}^D_{m-loop} = \int \prod_{i=1}^{m} \frac{d^D \ell_i}{\ell_i^2} \mathcal{I}^{(D+d)}_{m-loop} \tag{3.11}$$

with

$$\mathcal{I}^{(D+d)}_{m-loop} = \int \frac{\left(\prod_{i=1}^{n+2m} dz_i\right)}{d\omega} \left(z_{ij} z_{jk} z_{ki} \prod_{a\neq i,j,k}^{n+2m} \delta\left(\mathcal{S}_a\right) \right) \mathcal{I}^{CHY} \ . \tag{3.12}$$

Let us give some explanations for (3.11) and (3.12). First although loop momenta in (3.11) are in D-dimension, when we use the CHY-formula to calculate $\mathcal{I}^{(D+d)}_{m-loop}$ as given in (3.12), we should treat loop momenta as massless in $(D+d)$-dimension as explained above. Thus we use notation $(D+d)$ to emphasize this point. Secondly, the formula (3.12) is the familiar tree-level CHY formula with $(n+2m)$-points, where $d\omega = \frac{dz_r dz_s dz_t}{z_{rs} z_{st} z_{tr}}$ comes from gauge fixing of three locations of z's by $SL((2,C)$ symmetry. While other part is universal for all theories, the CHY-integrand $\mathcal{I}^{CHY}$ is the one distinguishing different theories. Thus our main focus will be the construction of $\mathcal{I}^{CHY}$.

The construction of CHY-integrands needs to satisfy some constraints. One of the most important constraints is the Mobius invariance. To compensate the variation of measure part in (3.12), under the $SL(2,C)$ transformation, $\mathcal{I}^{CHY}$ should have following transformation property

$$\mathcal{I}^{CHY} \to \left(\prod_{i=1}^{n+2m} \frac{(ad-bc)^2}{(cz_i+d)^4} \right)^{-1} \mathcal{I}^{CHY} \ . \tag{3.13}$$

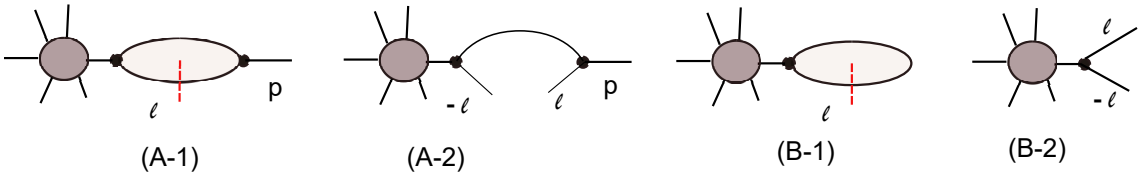

Figure 3: The excluded one-loop Feynman diagrams of ϕ^3 theory and their corresponding trees after the cut

A nice way to satisfy above transformation property is to construct various combinations carrying different weights as demonstrated in [1, 2, 3, 4, 5]. Two familiar factors with weight two are (more factors can be found in [4, 5])

$$C_{U(N)}(z) = \left(\sum_{\alpha \in S_n/Z_n} \frac{\mathrm{Tr}(T^{\alpha(1)}...T^{\alpha(n)})}{z_{\alpha(1)\alpha(2)}\cdots z_{\alpha(n-1)\alpha(n)} z_{\alpha(n)\alpha(1)}} \right), \qquad E(\epsilon, k, z) = (\mathrm{Pf}'\Psi(k, \epsilon, z). \tag{3.14}$$

Besides the weight conditions, there are other physical considerations, such as the soft limit, the factorization property etc.

Although using the idea of dimension reduction, we have mapped the loop problem to tree one in (3.12), the CHY-integrand $\mathcal{I}^{CHY}$ are not exactly the tree-level CHY integrands we are familiar with. There are two main reasons. The first one is that since tree-level Feynman diagrams are obtained by cutting internal lines, there are many choices of which lines have been cut, thus one needs to sum over all allowed insertions of $2m$ extra legs (and possible summing over polarization states of extra legs if particles running along the loop are not scalars). This phenomenon has been discussed for one-loop cases in [41, 42, 43, 44]. The second reason is more crucial: *after cutting loop diagrams to trees, we do not get all allowed tree-level diagrams of* $(n+2m)$*-points*. For example, for one-loop amplitude of massless theories, there are two kinds of diagrams we need to exclude: the tadpole diagrams (B-1) in Figure 3 and the massless bubble diagrams (A-1) in Figure 3. After reducing loop diagrams to trees, we should exclude these diagrams (A-2), (B-2) in Figure 3 from allowed tree-level diagrams. These two kinds of tree diagrams are singular under the forward limit. Thus the true CHY-integrand in (3.12) should be the one from trees after subtracting these divergent parts.

However, the subtracting of these singular parts is very nontrivial. For some theories, for example, the supersymmetric theory, it has been shown in [51] that the singular forward limit disappears by supersymmetry[2], so we do not need to worry about it. However, for pure Yang-Mills theory, the subtracting in the CHY frame is not completely clear. Since these subtleties, in this paper we will focus on planar loop integrands of color ordered bi-adjoint scalar ϕ^3 theory. Although the theory is simple, it is good enough for our one main purpose of the paper, i.e., to find the generalization of powerful mapping rule between CHY-integrands and Feynman diagrams given in [30, 31, 41] at the tree-level and one-loop level.

[2]For other massless theories, recent $\mathcal{Q}$-cut construction in [45] has given a way to remove forward singularities by using the scale deformation.

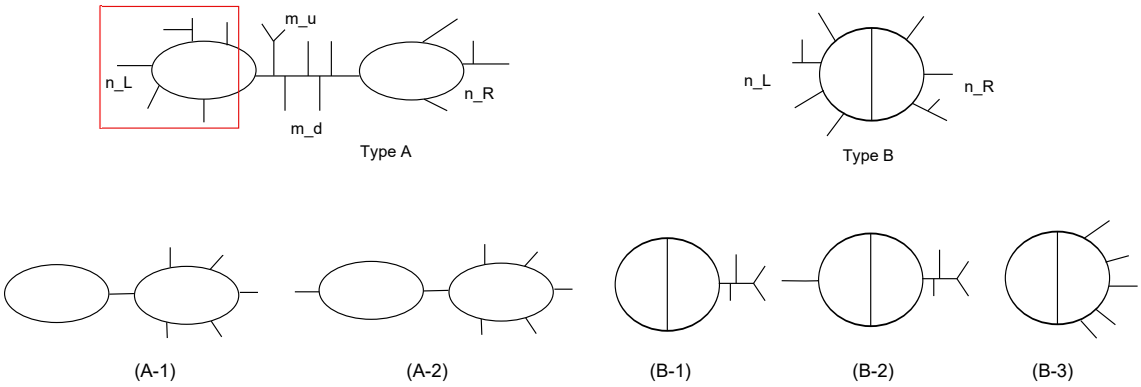

Figure 4: General planar two-loop Feynman diagrams Type (A) and Type (B) of ϕ^3 theory. There are some special two-loop diagrams: (A-1) one-loop tadpole; (A-2) one-loop massless bubble; (B-1) two-loop tadpole; (B-2) two-loop massless bubble; and (B-3) Reducible two-loop diagrams.

4. Two-loop CHY-integrand of ϕ^3 theory

Having discussed all loop scattering equations, now we discuss how to write down all loop CHY-integrands in (3.12), at least for planar part of color ordered bi-adjoint ϕ^3 theory. For simplicity, we will use the two-loop example to demonstrate our strategy, but the idea should be easily generalized to all loops. The key strategy to loop CHY-integrands is to use the mapping rule found in papers [30, 31, 41]. Using the mapping rule, if we know what is expressions from field theory side through Feynman diagrams, we could find the corresponding CHY-integrands.

4.1 Analysis of two-loop Feynman diagrams

Having above strategy, now we start to analyze color ordered two-loop planar integrands obtained from Feynman diagrams. To have a clear picture of these integrands, let us start with the classification of planar two-loop Feynman diagrams of ϕ^3 theory. It is easy to see that all diagrams are divided into two types, i.e., type (A) and type (B) (see Figure 4). The type (A) is the relative trivial one as it is given by two sub-oneloop diagrams. For these diagrams, we will use $T_{(n_L;m_u,m_d;n_R)}$ to denote them, where n_L, n_R, m_u, m_d are number of external legs attached to the left sub-oneloop, right sub-oneloop, the upper part of the middle line and the lower part of middle line. The type (B) is the really nontrivial two-loop diagram with one mixed propagator. For these diagrams, we will use $T_{(n_L;n_R)}$ to denote them, where n_L, n_R are numbers of external legs attached to the left part and right part.

Among these diagrams given in Figure 4, there are some singular two-loop diagrams, for which we will have more careful discussions. They are (see Figure 4):

- When one of n_L or n_R of Type (A) is zero, we have one-loop tadpole structure as given by (A-1).

- When one n_L or n_R of Type (A) is one and all other external legs are grouped together to attach to another loop by only one vertex, we have one-loop massless bubble structure as given by (A-2).

- When n_L or n_R of Type (B) are zero , we get the reducible two-loop structure as given by (B-3). For the case (B-3), when all external legs are grouped together to attach to the loop by only one vertex, we get the two-loop tadpole structure as given by (B-1).

- When one of n_L and n_R of Type (B) is one and all other external legs are grouped together to attach to another loop by only one vertex, we get the two-loop massless bubble structure as given by (B-2).

From general two-loop Feynman diagrams, we see that two-loop integrands should be the sum of terms of following two types[3] (see the diagrams (A) and (B) in Figure 4)

$$\begin{aligned}\mathcal{I}_A &= \frac{1}{\mathcal{E}\,(\prod_i(\ell_1+K_i)^2)\,(\prod_s(\ell_2+K_s)^2)}\\ \mathcal{I}_B &= \frac{1}{\mathcal{E}\,(\prod_i(\ell_1+K_i)^2)\,(\prod_s(\ell_2+K_s)^2)\,(\ell_1-\ell_2+R)^2}\end{aligned} \tag{4.1}$$

where $\mathcal{E}$ is the product of poles involving only external momenta. To proceed, just like the one-loop case [22, 41], we do the partial fraction using following identity[4]

$$\frac{1}{\prod_{i=1}^n D_i} = \sum_{i=1}^n \frac{1}{D_i \prod_{j\neq i}(D_j - D_i)} \tag{4.2}$$

and then make loop momenta shifting. For the type $\mathcal{I}_A$, the partial fraction and loop momentum shifting will give the standard form $\frac{1}{\ell_1^2\ell_2^2}\frac{1}{\prod P_i}$ with pole P_i's having following combinations like $2\ell_i\cdot(K_j-K_i)+(K_j-K_i)^2 = [\ell_i, k_{t_1}, ..., k_{t_m}]$ (see the notation (2.1)) if $K_j - K_i = \sum_{i=1}^m k_{t_i}$. These poles are the familiar ones appearing in the mapping rule (2.2) [5] at the tree and one-loop levels. Thus it will be not so surprising that using the same mapping rule reviewed in the section two we can easily read out corresponding expressions given a CHY-integrand.

However, for the type $\mathcal{I}_B$, things are not so simple because now we have a mixed propagator[6] $(\ell_1 - \ell_2 + R)^2$. When we do the partial fraction of ℓ_1, should we include the mixed propagator $(\ell_1 - \ell_2 + R)^2$ in (4.2) or not? It is easy to see that if we include the mixed propagator, then we will have terms like $\frac{1}{(\ell_1-\ell_2+R)^2}\frac{1}{\prod_i((\ell_1+K_i)^2-(\ell_1-\ell_2+R)^2)}$. To have the standard $\frac{1}{\ell_1^2\ell_2^2}$ factor in (3.11), we need to shift $\ell_1 = \widehat{\ell}_1+\ell_2-R$. Although it is nothing wrong with this manipulation, the ending pole $((\ell_1+K_i)^2-(\ell_1-\ell_2+R)^2)$

[3] Under our convention, the color ordering is clockwise. All external momenta are incoming while loop momenta will run along clockwise direction, so when we cut inner propagator ℓ between the leg 1 and the leg 2, we should have the ordering as $(1, -\ell, \ell, 2)$, i.e, *moving along the clockwise direction is translated to moving from the left to the right*. Furthermore, the nontrivial mixed propagator will have the momentum $(\ell_1 - \ell_2 + R)^2$.

[4] The integrand of the type (B-3) in Figure 4 is given by $\frac{1}{\ell_1^2(\prod_{i=1}^m(\ell_1+P_i)^2)\ell_1^2(\ell_1-\ell_2)^2\ell_2^2}$. The appearance of $(\ell_1^2)^2$ will make the application of partial fraction tricky. We will discuss these contributions later. Similar thing happens to the type (A-1).

[5] It is also worth to notice that it is these contractions $2k_i\cdot k_j$ appearing in the numerator of scattering equations.

[6] For two-loop planar diagram, there is at most one mixed propagator.

will become $2\widehat{\ell}_1\cdot(\ell_2-R+K)^2+(\ell_2-R+K)^2$, where although we have linearized the $\widehat{\ell}_1$, the ℓ_2^2 will appear. The appearance of ℓ_2^2 will make the next partial fraction of ℓ_2 very complicated. Furthermore, the mapping rule succussed at the tree and one-loop levels can not cooperate the term ℓ_2^2. To avoid these troubles, one possible way is to exclude the mixed propagator when we do the partial fraction over both loop momenta ℓ_1 and ℓ_2, then we will arrive the sum of terms like $\frac{1}{\ell_1^2\ell_2^2(\ell_1-\ell_2+R)^2\prod_i\prod_{j=1,2}[\ell_j,k_{i_1},\ldots,k_{i_m}]}$. Although the linearized poles fit to the mapping rule, the remaining mixed propagator $(\ell_1-\ell_2+R)^2$ does not.

Is there a frame such that both features mentioned in previous paragraph (i.e., the partial fraction without the mixed propagator and the applicability of the mapping rule) can be preserved? The answer is yes if we lift the massive loop momenta in D-dimension to massless loop momenta in $(D+d)$-dimension as discussed in previous section. As discussed in the paper [45], the procedure of partial fraction can be understood as taking the residue of poles containing dimensional deformed loop momenta. More explicitly, let us deform the loop momenta from D-dimension to $(D+d)$-dimension $\ell_i\to\widetilde{\ell}_i=\ell_i+\eta_i$. Under this deformation, we have

$$(\ell_i+P)^2\to(\widetilde{\ell}_i+P)^2=(\ell_i+P)^2-\eta_i^2\equiv(\ell_i+P)^2+z_i \tag{4.3}$$

as well as

$$(\ell_1-\ell_2+R)^2\to(\widetilde{\ell}_1-\widetilde{\ell}_2+R)^2=(\ell_1-\ell_2+R)^2-(\eta_1-\eta_2)^2 \tag{4.4}$$

As long as $d\geq 2$, we have the freedom to make different choices for $(\eta_1-\eta_2)^2$ while keeping $-\eta_i^2=z_i$ invariant. In [45], the choice made is that $-(\eta_1-\eta_2)^2=z_3$ as a new independent variable, while for current paper, we will make the choice $-(\eta_1-\eta_2)^2=0$. This can be achieved, for example, taking

$$\eta_1=(x+iy,x-iy),\quad \eta_2=(ix+z,ix-z) \tag{4.5}$$

with

$$\left\{x=-\frac{i(z_1-z_2)}{\sqrt{(8+8i)z_1-(8-8i)z_2}},y=-\frac{i((2+i)z_1+iz_2)}{\sqrt{(8-8i)z_2-(8+8i)z_1}},z=\frac{z_1+(1+2i)z_2}{2\sqrt{2}\sqrt{(-1-i)(z_1+iz_2)}}\right\} \tag{4.6}$$

thus $(\eta_1-\eta_2)^2=0$ for all z_1,z_2. Under this choice

$$\begin{aligned}\mathcal{I}_B(z_1,z_2)&=\frac{1}{\mathcal{E}(\ell_1-\ell_2+R)^2}T_1(z_1)T_2(z_2),\\ T_1(z_1)&=\frac{1}{\prod_i((\ell_1+K_i)^2+z_1)},\qquad T_2(z_2)=\frac{1}{\prod_s((\ell_2+K_s)^2+z_2)}\ .\end{aligned} \tag{4.7}$$

It is easy to see that using the contour integration $\oint\frac{dz_1}{z_1}T_1(z_1)$ we can write down[7]

$$\begin{aligned}T_1(z_1=0)&=\sum_i\frac{1}{(\ell_1+K_i)^2}\frac{1}{\prod_{j\neq i}((\ell_1+K_j)^2-(\ell_1+K_i)^2)}\\&\sim\sum_i\frac{1}{\ell_1^2}\frac{1}{\prod_{j\neq i}(2\ell_1\cdot(K_j-K_i)+(K_j-K_i)^2)}\end{aligned} \tag{4.8}$$

[7]For this simple case, there is no residue at $z_1=\infty$.

where at the second line we have shifted the loop momentum to become standard form, which is legitimate under the proper regularization of loop integration (such as the dimensional regularization). Similar expression for $T_2(z_2 = 0)$ can be written down too. Above manipulation is nothing, but the partial fraction where the mixed propagator $(\ell_1 - \ell_2 + R)^2$ is not touched, which is exactly what we want. Furthermore, locations of poles impose on-shell conditions $\widetilde{\ell}_i^2 = 0$, $i = 1, 2$, thus the mixed propagator can be written as

$$(\ell_1 - \ell_2 + R)^2 = (\widetilde{\ell}_1 - \widetilde{\ell}_2 + R)^2 = -2\widetilde{\ell}_1 \cdot \widetilde{\ell}_2 + R^2 + 2R \cdot (\widetilde{\ell}_1 - \widetilde{\ell}_2) = [\widetilde{\ell}_1, -\widetilde{\ell}_2, r_1, ..., r_m], \quad R = \sum_i k_{r_i} \tag{4.9}$$

which is exactly the right pole structure given in the mapping rule (2.2).

Overall, under this new perspective, the two-loop planar integrand can be written as the sum of following terms[8]

$$\frac{1}{\ell_1^2 \ell_2^2} \left\{ \sum_{i,s} \frac{1}{\widetilde{\mathcal{E}} \prod_{j \neq i} [\widetilde{\ell}_1, K_j - K_i] \prod_{t \neq s} [\widetilde{\ell}_2, K_t - K_s]^2} \right\} |_{\widetilde{\ell}_1^2 = \widetilde{\ell}_2^2 = 0} \tag{4.10}$$

where $\widetilde{\mathcal{E}}$ is $\mathcal{E}$ for $\mathcal{I}_A$ and $\mathcal{E}[\widetilde{\ell}_1, -\widetilde{\ell}_2, R]$ for $\mathcal{I}_B$. From (4.10) it is clear that the calculation of two-loop integrands is reduced to the calculation of the part inside the curly bracket. What is the physical picture of these terms? The on-shell conditions $\widetilde{\ell}_1^2 = \widetilde{\ell}_2^2 = 0$ mean that we have cut two loop momenta to on-shell, thus two-loop diagrams are open up to become tree diagrams with 4 extra legs with momenta $-\widetilde{\ell}_1, \widetilde{\ell}_1, -\widetilde{\ell}_2, \widetilde{\ell}_2$. However, as we have discussed before, not all tree diagrams with $(n + 4)$-legs can be obtained by this way, especially these coming from one-loop and two tadpoles and one-loop and two-loop massless bubbles (see Figure 4). We will discuss this problem in next subsection.

4.2 Special Feynman diagrams

In this subsection, we focus on these special diagrams given in Figure 4. Among them, tadpoles and massless bubbles are singular, thus we should remove corresponding contributions of these tree diagrams, obtained after cutting two internal propagators from these singular two-loop diagrams, from (4.10). To be able to do so, we need to have a better understanding of these tree diagrams.

Let us start from the one-loop tadpoles (A-1) and one-loop massless bubbles (A-2) in Figure 4. Depending on if the left sub-oneloop or right sub-oneloop are tadpoles or massless bubbles, we have four different combinations, which are given by four boxed corners in Figure 5. For the upper-left corner, it is the left sub-oneloop having tadpole structure while the right sub-oneloop can have arbitrary structure. After cutting two loop propagators, we get corresponding tree diagrams with $(n + 4)$-legs. However, all these diagrams have a common feature: all of them contain the pole $s_{(-\ell_1)\ell_1}$. We will call it the "**signature**" of tadpole structure. For the lower-right corner, the left sub-oneloop has the massless bubble structure while the right sub-oneloop can have arbitrary structure. After cutting two loop propagators, we

[8] Again the form (4.10) can not contain contributions from the reducible two-loop diagrams (see type (B-3) in Figure 4), for which we will discuss separately.

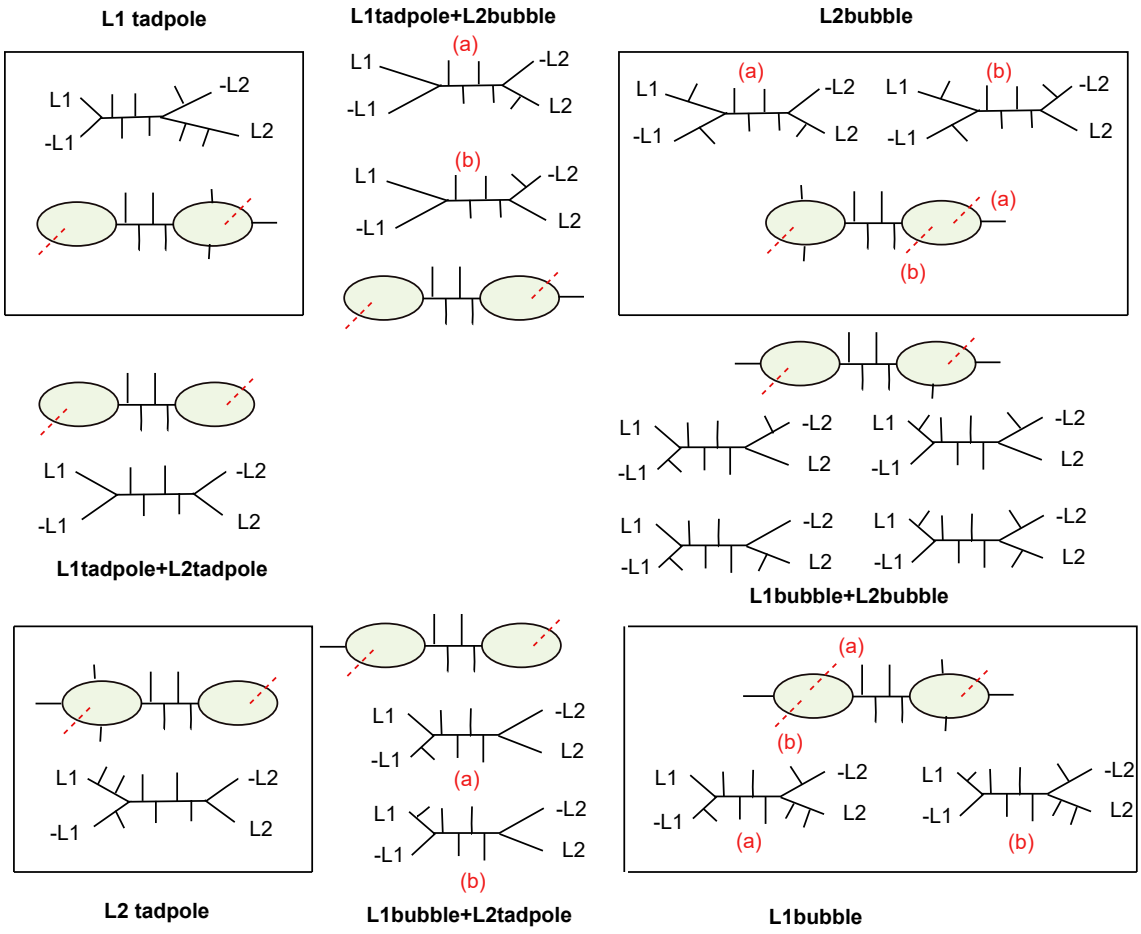

Figure 5: Singular contributions from the one-loop tadpoles and one-loop massless bubbles. At the four corners, we have four general cases. For example, the corner "L1-tadpole" means that the left one-loop is tadpole while the right one-loop can be general. Each pair of nearby corners has an intersection. For example, between the corner "L1-tadpole" and the corner "L2-bubble" we will have the diagram where the left one-loop is tadpole and the right one-loop is massless bubble. For each loop diagram, we have also drawn the corresponding tree diagrams after the cut. These pictures will be very useful when we discuss how to write down the CHY-integrand.

get corresponding tree diagrams having following "signature" of massless bubble structure: either having pole $s_{(-\ell_1)p}s_{(-\ell_1)\ell_1 p}$ or having pole $s_{\ell_1 p}s_{(-\ell_1)\ell_1 p}$ with p, the massless leg. Similar analysis can be done for the upper-right corner where the right sub-oneloop has the massless bubble structure and the lower-left corner where the right sub-oneloop has the tadpole structure.

Above four corners have included all singular behaviors for sub-oneloop structure in two-loop diagrams. However, they are not completely separate from each other. For example, we can have the special case where both left and right sub-oneloops have the tadpole structure. This has been given in the middle between the upper-left corner and the lower-left corner in Figure 5. The signature of corresponding tree

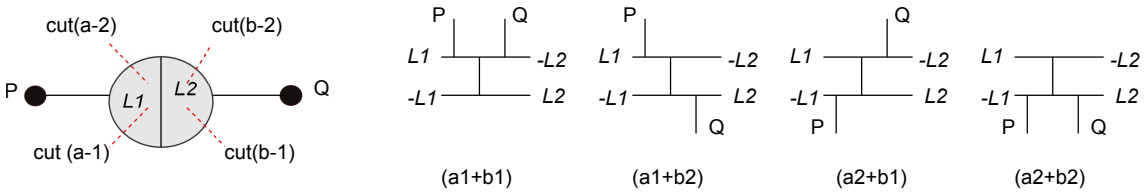

Figure 6: The two-loop massless bubble and its corresponding tree diagrams after various combinations of cuts.

diagrams is the appearance of poles $s_{(-\ell_1)\ell_1}$ and $s_{(-\ell_2)\ell_2}$ at same time. Similar phenomena happens for each pair of corners near each other and we have listed them all in Figure 5.

Having understood the one-loop tadpole and massless bubble singularities, we move to the two-loop tadpole and massless bubble singularities. For two-loop massless bubble given in Figure 6, depending on different combinations of cuts, we have four different tree diagrams. Among these four cases, the forward pairs $(-\ell_1, \ell_1)$ and $(-\ell_2, \ell_2)$ are next to each other only in two cases. The signature of these four cases are $s_{(-\ell_1)\ell_2}s_{P\ell_1}s_{Q(-\ell_2)}$, $s_{Q(-\ell_1)\ell_2}s_{P\ell_1}s_{Q\ell_2}$, $s_{p(-\ell_1)\ell_2}s_{P(-\ell_1)}s_{Q(-\ell_2)}$ and $s_{\ell_1(-\ell_2)}s_{P(-\ell_1)}s_{Q\ell_2}$ with $P+Q=0$. Furthermore, depending upon if P or Q are massless particle, we need to add another pole s_P or s_Q.

To discuss the two-loop tadpole, let us start with the (B-3) in Figure 4. Since all external legs are attached to one side, the integrand will have the form (see the (A-1) of Figure 7)

$$\frac{1}{\ell_1^2(\prod_{i=1}^m(\ell_1+P_i))\ell_1^2(\ell_1-\ell_2)^2\ell_2^2}\ , \tag{4.11}$$

where the appearance of $(\ell_1^2)^2$ makes the naive application of partial fraction to (4.1) problematically. Thus we should not expect to reduce these contributions to the form (4.10). Then how to deal with them? One hint is to rearrange (4.11) as

$$\frac{1}{\ell_1^2(\ell_1-\ell_2)^2\ell_2^2}\left\{\frac{1}{\ell_1^2(\prod_{i=1}^m(\ell_1+P_i))}\right\}\ , \tag{4.12}$$

then the part inside the bracket is nothing, but the familiar one-loop integrand. However, there is one subtle point regarding to the choice of loop momentum ℓ_1. With the convention given in (A-1) and (A-2) of Figure 7, it is easy to see that although when rewriting to the form (4.12), both produce one-loop integrands with the same color ordering, these two one-loop integrands are not same since they have different conventions of loop momentum ℓ_1 inherited from two-loop diagrams (although they are related by loop momentum shifting). With above understanding, we can write two-loop integrands coming from the type (B-3) in Figure 4 as

$$\mathcal{I}_{B_3}^{2-loop}=\left\{\frac{1}{\ell_1^2(\ell_1-\ell_2)^2\ell_2^2}\left\{\mathcal{I}^{1-loop}(1,2,...,n,\ell_1)+\text{cyclic permu}\{1,2,...,n\}\right\}\right\}+\{\ell_1\leftrightarrow\ell_2\} \tag{4.13}$$

Now we give some explanations for (4.13). First, in each one-loop diagram of $\mathcal{I}^{1-loop}(1,2,...,n,\ell_1)$, the loop propagator at the right of the vertex where leg 1 has connected to is defined to be ℓ_1. Secondly, the

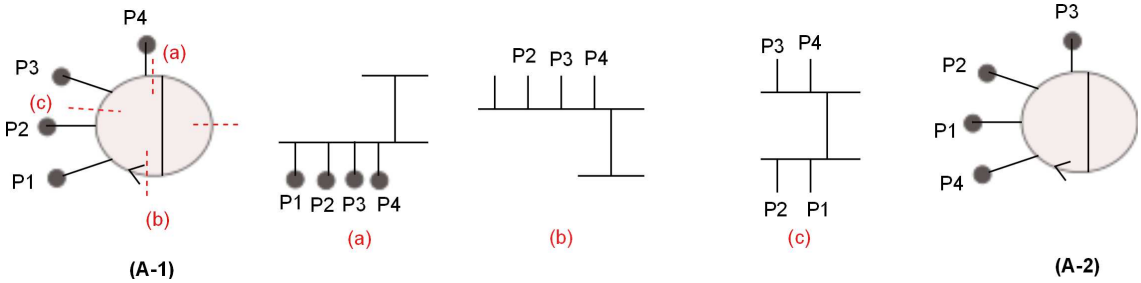

Figure 7: The reducible two-loop diagram (A-1) and its corresponding tree diagrams (a), (b), (c) after cuts. The two-loop diagram (A-2) are obtained from (A-1) by a cyclic permutation. (A-1) and (A-2) give different contributions and we should sum over all cyclic permutations, plus the symmetrization between ℓ_1, ℓ_2.

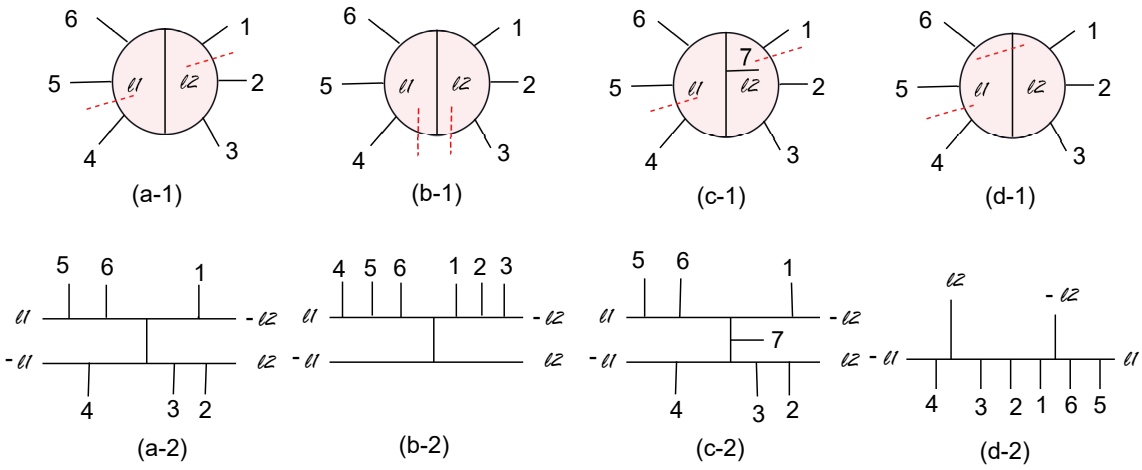

Figure 8: Planar two-loop diagrams with two cuts and their corresponding color ordered tree diagrams. In (a),(b), $-\ell_i, \ell_i$ are next to each other while in (c), (d) it is not true anymore.

two-loop tadpole diagram (B-1) in Figure 4 is reduced to the one-loop tadpole diagram, thus if we exclude these contributions from tadpole diagrams in $\mathcal{I}^{1-loop}(1,2,...,n,\ell_1)$, we have excluded the two-loop tadpole contributions. Thirdly, since we have reduced the calculation of $\mathcal{I}_{B_3}^{2-loop}$ to one-loop case, we can take them as known data. Thus when we try to find the CHY-construction of two-loop integrands in (4.10), we can exclude $\mathcal{I}_{B_3}^{2-loop}$ part. The complete planar two-loop integrand will be the sum of the result (4.10) and the result (4.13). This will be the strategy we follow in the later part of the paper although in the subsection 4.4 we do give a CHY-construction of the $\mathcal{I}_{B_3}^{2-loop}$ part as the soft limit of a corresponding theory with $(n+5)$-points.

4.3 The construction of CHY-integrand

Having reduced the problem of finding loop integrands to tree diagrams in (4.10) (after excluding the

$\mathcal{I}_{B_3}^{2-loop}$ part), we need to determine which tree diagrams we should consider. Since these tree diagrams are obtained from planar two-loop diagrams by cutting two internal propagators, we can get general picture by speculating the Figure 8. By checking different combinations of two cuts, such as these in (a-1) and (b-1), we can see that in the resulted color ordered tree diagrams (such as these in (a-2) and (b-2)), $-\ell_1$ is always next to ℓ_1 (similar for the pair $-\ell_2, \ell_2$). This pattern does not hold anymore for non-planar two-loop diagrams (see (c-2)) or cutting along the mixed propagator (see (d-2)). Using this observation, we conclude that the resulted tree diagrams are these obtained from the original color ordered n-point tree diagrams after inserting two pairs $(-\ell_i, \ell_i)$ consistently to all possible locations. More explicitly, we will have following two types of ordered diagrams with $(n+4)$-points:

- Type (I): there are $2n$ of them having following ordering

$$\mathcal{O}_j \equiv \{1, ..., j, (-\widetilde{\ell}_1, \widetilde{\ell}_1), (-\widetilde{\ell}_2, \widetilde{\ell}_2), j+1, ..., n\} \tag{4.14}$$

  where $j = 1, 2, ..., n$ (plus also the symmetrization of $\widetilde{\ell}_1 \leftrightarrow \widetilde{\ell}_2$)[9].

- Type (II): there are $n(n-1)$ of them having following ordering

$$\mathcal{O}_{jk} \equiv \{1, ..., j, (-\ell_1, \ell_1), j+1, ..., k, (-\ell_2, \ell_2), k+1, ..., n\} \tag{4.15}$$

  with $1 \leq j < k \leq n$ (plus also the symmetrization of $\widetilde{\ell}_1 \leftrightarrow \widetilde{\ell}_2$).

Having found related color ordered tree amplitudes, we know immediately that the part inside the bracket of (4.10) is the sum of these color ordered tree level amplitudes of type (I) and (II), after removing possible forward singularities and the $\mathcal{I}_{B_3}^{2-loop}$ part contained in them. Thus the wanted CHY-integrand $\mathcal{I}^{CHY}$ in (3.12) should produce these contributions. To find it, we need to use the mapping rule established in [30, 31, 41]. Now we discuss one by one.

4.3.1 The CHY-integrand for ordering $\mathcal{O}_{jk}$

Having above general discussions, now we determine the CHY-integrand for each ordering in (4.14) and (4.15). Let us start with the ordering $\mathcal{O}_{jk}$. With this ordering, the full tree-level amplitude is given by following CHY-integrand

$$T_{jk} = \frac{1}{z_{12}^2 ... z_{j(-\ell_1)}^2 z_{(-\ell_1)\ell_1}^2 z_{\ell_1(j+1)}^2 ... z_{k(-\ell_2)}^2 z_{(-\ell_2)\ell_2}^2 z_{\ell_2(k+1)}^2 ... z_{n1}^2} \ . \tag{4.16}$$

Now we consider various forward limits, which can be produced in this ordering. For this purpose, the Figure 5, the Figure 6 and the Figure 7 are very useful. From these Figures, we see that this ordering can contain following singularities:

[9]The symmetrization is necessary since there is no canonical definition of two loops.

- First it can contain the ℓ_1-tadpole singularity, i.e., with pole $s_{(-\ell_1)\ell_1}$. These tree diagrams are obtained by the CHY-integrand (please see the Appendix A for full explanations)

$$T_{jk;t_1} = \frac{1}{z_{12}^2 ... z_{j(-\ell_1)} \underline{z_{j\ell_1}} z_{(-\ell_1)\ell_1}^2 \underline{z_{(-\ell_1)(j+1)}} z_{\ell_1(j+1)} ... z_{k(-\ell_2)}^2 z_{(-\ell_2)\ell_2}^2 z_{\ell_2(k+1)}^2 ... z_{n1}^2} \tag{4.17}$$

where we use the t_1 to denote the ℓ_1-tadpole singularity and the underline to emphasize the changed factor. We can write (4.17) to more compact way by using the rule (2.11)

$$T_{jk;t_1} = T_{ij}\mathcal{P}[j, -\ell_1, \ell_1, j+1] \ . \tag{4.18}$$

- Secondly it contains massless ℓ_1-bubble singularities, i.e., these given by pole structures $s_{j(-\ell_1)}s_{j(-\ell_1)\ell_1}$ or $s_{\ell_1(j+1)}s_{(-\ell_1)\ell_1(j+1)}$. Using the rule (2.11) we can write down the corresponding CHY-integrands as

$$T_{jk;b_1 j} = T_{jk}\mathcal{P}[j-1, j, -\ell_1, \ell_1]\mathcal{P}[j-1, j, \ell_1, j+1] \tag{4.19}$$

and

$$T_{jk;b_1(j+1)} = T_{jk}\mathcal{P}[-\ell_1, \ell_1, j+1, j+2]\mathcal{P}[j, -\ell_1, j+1, j+2] \tag{4.20}$$

where we use b_1 for massless bubble involving the ℓ_1 and j to denote the massless bubble of j-th leg. We want to emphasize one thing: above three singularities are not compatible, i.e., they can not appear at same time in a given tree diagram. Thus when we subtract their contributions, we should subtract all of them.

- Similar considerations can be done for the ℓ_2 part and we get following three CHY-integrands

$$T_{jk;t_2} = T_{ij}\mathcal{P}[k, -\ell_2, \ell_2, k+1] \tag{4.21}$$

$$T_{jk;b_2 k} = T_{jk}\mathcal{P}[k-1, k, -\ell_2, \ell_2]\mathcal{P}[k-1, k, \ell_2, k+1] \tag{4.22}$$

$$T_{jk;b_2(k+1)} = T_{jk}\mathcal{P}[-\ell_2, \ell_2, k+1, k+2]\mathcal{P}[k, -\ell_2, k+1, k+2] \tag{4.23}$$

corresponding to one-loop tadpoles and one-loop massless bubbles of ℓ_2-loop.

- Now coming to an important observation: the one-loop tadpole and one-loop massless bubble singularities of ℓ_1 are (almost) compatible with the one-loop tadpole and one-loop massless bubble singularities of ℓ_2. Thus we will have following nine CHY-integrands to describe tree diagrams having both kinds of singularities. They are:

$$T_{jk;t_1,t_2} = T_{ij}\mathcal{P}[j, -\ell_1, \ell_1, j+1]\mathcal{P}[k, -\ell_2, \ell_2, k+1] \ , \tag{4.24}$$

$$T_{jk;t_1,b_2 k} = T_{jk}\mathcal{P}[j, -\ell_1, \ell_1, j+1]\mathcal{P}[k-1, k, -\ell_2, \ell_2]\mathcal{P}[k-1, k, \ell_2, k+1] \ , \tag{4.25}$$

$$T_{jk;t_1,b_2(k+1)} = T_{jk}\mathcal{P}[j, -\ell_1, \ell_1, j+1]\mathcal{P}[-\ell_2, \ell_2, k+1, k+2]\mathcal{P}[k, -\ell_2, k+1, k+2] \ , \tag{4.26}$$

and

$$T_{jk;b_1 j,t_2} = T_{ij}\mathcal{P}[j-1,j,-\ell_1,\ell_1]\mathcal{P}[j-1,j,\ell_1,j+1]\mathcal{P}[k,-\ell_2,\ell_2,k+1]\ , \tag{4.27}$$

$$T_{jk;b_1 j,b_2 k} = T_{jk}\mathcal{P}[j-1,j,-\ell_1,\ell_1]\mathcal{P}[j-1,j,\ell_1,j+1]\mathcal{P}[k-1,k,-\ell_2,\ell_2]\mathcal{P}[k-1,k,\ell_2,k+1]\ , \tag{4.28}$$

$$\begin{aligned} T_{jk;b_1 j,b_2(k+1)} = & T_{jk}\mathcal{P}[j-1,j,-\ell_1,\ell_1]\mathcal{P}[j-1,j,\ell_1,j+1]\mathcal{P}[-\ell_2,\ell_2,k+1,k+2] \\ & \mathcal{P}[k,-\ell_2,k+1,k+2]\ , \end{aligned} \tag{4.29}$$

and

$$T_{jk;b_1(j+1),t_2} = T_{ij}\mathcal{P}[-\ell_1,\ell_1,j+1,j+2]\mathcal{P}[j,-\ell_1,j+1,j+2]\mathcal{P}[k,-\ell_2,\ell_2,k+1]\ , \tag{4.30}$$

$$\begin{aligned} T_{jk;b_1(j+1),b_2 k} = & T_{jk}\mathcal{P}[-\ell_1,\ell_1,j+1,j+2]\mathcal{P}[j,-\ell_1,j+1,j+2]\mathcal{P}[k-1,k,-\ell_2,\ell_2] \\ & \mathcal{P}[k-1,k,\ell_2,k+1]\ , \end{aligned} \tag{4.31}$$

$$\begin{aligned} T_{jk;b_1(j+1),b_2(k+1)} = & T_{jk}\mathcal{P}[-\ell_1,\ell_1,j+1,j+2]\mathcal{P}[j,-\ell_1,j+1,j+2]\mathcal{P}[-\ell_2,\ell_2,k+1,k+2] \\ & \mathcal{P}[k,-\ell_2,k+1,k+2]\ . \end{aligned} \tag{4.32}$$

There is one warning: when there is only one leg between two pairs of loop momenta, among above nine combinations, some combinations can not exist. More explicitly, when $k = j+1$, the combination $T_{jk;b_1(j+1),b_2 k}$ can not exist, while when $k = n, j = 1$ the combination $T_{jk;b_1 j,b_2(k+1)}$ can not exist.

The reason to discuss the compatible structure is to not overly subtract the singular part. For example, after we subtract $T_{jk;t_1}$ and $T_{jk;t_2}$ from T_{jk}, the part $T_{jk;t_1,t_2}$ has been subtracted two times, thus we need to add the $T_{jk;t_1,t_2}$ part to compensate.

- Having excluded one-loop singularities, we continue to remove two-loop massless bubble singularities. Although a little bit of away from our concern, let us start with the bubble structure (so including the massive bubble). From the Figure 6, we see that two-loop bubble structure will have five fixed poles. With the signature $s_{(j+1)\ldots k}s_{\ell_1(j+1)\ldots k}s_{(k+1)\ldots j}s_{\ell_2(k+1)\ldots j}s_{\ell_2(k+1)\ldots j(-\ell_1)}$ the corresponding CHY-integrand is

$$\begin{aligned} T_{jk;2m1} = & T_{jk}\mathcal{P}[\ell_1,j+1,k,-\ell_2]\mathcal{P}[-\ell_1,\ell_1,k,-\ell_2]\mathcal{P}[\ell_2,k+1,j,-\ell_1] \\ & \mathcal{P}[-\ell_2,\ell_2,j,-\ell_1]\mathcal{P}[-\ell_2,\ell_2,-\ell_1,\ell_1] \end{aligned} \tag{4.33}$$

while with the signature $s_{(j+1)\ldots k}s_{(j+1)\ldots k(-\ell_2)}s_{(k+1)\ldots j}s_{(k+1)\ldots j(-\ell_1)}s_{\ell_2(k+1)\ldots j(-\ell_1)}$ the corresponding CHY-integrand is

$$\begin{aligned} T_{jk;2m2} = & T_{jk}\mathcal{P}[\ell_1,j+1,k,-\ell_2]\mathcal{P}[\ell_1,j+1,-\ell_2,\ell_2]\mathcal{P}[\ell_2,k+1,j,-\ell_1] \\ & \mathcal{P}[\ell_2,k+1,-\ell_1,\ell_1]\mathcal{P}[-\ell_2,\ell_2,-\ell_1,\ell_1] \end{aligned} \tag{4.34}$$

Above pole structures with five s-factors are general. To get the massless bubble, we need pole $s_{(j+1)\ldots k} = s_{(k+1)\ldots j}$ to be zero. This can happen only when $k = j+1$ or $k = n, j = 1$. For

$k = j+1$, the signature of $T_{jk;2m1}$ type reduces to $s_{\ell_1(j+1)\ldots k}s_{(k+1)\ldots j}s_{\ell_2(k+1)\ldots j(-\ell_1)}$ and the corresponding CHY-integrand is

$$T_{jk;2m1} = T_{jk}\mathcal{P}[-\ell_1,\ell_1,k,-\ell_2]\mathcal{P}[\ell_2,k+1,j,-\ell_1]\mathcal{P}[-\ell_2,\ell_2,j,-\ell_1]\mathcal{P}[-\ell_2,\ell_2,-\ell_1,\ell_1] \tag{4.35}$$

while the signature of $T_{jk;2m2}$ type reduces $s_{(j+1)\ldots k(-\ell_2)}s_{(k+1)\ldots j}s_{(k+1)\ldots j(-\ell_1)}s_{\ell_2(k+1)\ldots j(-\ell_1)}$ and the corresponding CHY-integrand is

$$T_{jk;2m2} = T_{jk}\mathcal{P}[\ell_1,j+1,-\ell_2,\ell_2]\mathcal{P}[\ell_2,k+1,j,-\ell_1]\mathcal{P}[\ell_2,k+1,-\ell_1,\ell_1]\mathcal{P}[-\ell_2,\ell_2,-\ell_1,\ell_1] \tag{4.36}$$

These two expressions (4.35) and (4.36) can be obtained from (4.33) and (4.34) by trivially setting $k = j+1$ since $\mathcal{P}[\ell_1,j+1,k,-\ell_2]|_{k=j+1} = 1$. Similarly for the case $k = n, j = 1$, the corresponding CHY-integrands can be also obtained from (4.33) and (4.34) by trivially setting $k = n, j = 1$ since $\mathcal{P}[\ell_2,k+1,j,-\ell_1]|_{k=n,j==1} = 1$.

These two are not compatible to each other. They are also not compatible with one-loop tadpole and one-loop massless bubble singularities.

- The last piece we need to exclude is the (B-3) part in Figure 4. From Figure 7, we see that with the signature $s_{\ell_1(j+1)\ldots k}s_{(k+1)\ldots j(-\ell_1)}s_{\ell_2(k+1)\ldots j(-\ell_1)}$ the corresponding CHY-integrand is

$$T_{jk;B31} = T_{jk}\mathcal{P}[-\ell_1,\ell_1,k,-\ell_2]\mathcal{P}[\ell_2,k+1,-\ell_1,\ell_1]\mathcal{P}[-\ell_2,\ell_2,-\ell_1,\ell_1] \tag{4.37}$$

while with the signature $s_{(j+1)\ldots k(-\ell_2)}s_{\ell_2(k+1)\ldots j}s_{\ell_2(k+1)\ldots j(-\ell_1)}$ the corresponding CHY-integrand is

$$T_{jk;B32} = T_{jk}\mathcal{P}[\ell_1,j+1,-\ell_2,\ell_2]\mathcal{P}[-\ell_2,\ell_2,j,-\ell_1]\mathcal{P}[-\ell_2,\ell_2,-\ell_1,\ell_1] \tag{4.38}$$

These two are not compatible to each other. They are also not compatible with one-loop tadpole, one-loop massless bubble and two-loop tadpole singularities.

Having above analysis, now we can write down the wanted CHY-integrand for the ordering $\mathcal{O}_{jk}$ as

$$\begin{aligned}\mathcal{I}^{CHY}_{\mathcal{O}_{jk}} = {} & T_{jk} - \big(T_{jk;t_1} + T_{jk;b_1j} + T_{jk;b_1(j+1)} + T_{jk;t_2} + T_{jk;b_2k} + T_{jk;b_2(k+1)}\big) \\ & + \big(T_{jk;t_1,t_2} + T_{jk;t_1,b_2k} + T_{jk;t_1,b_2(k+1)} + T_{jk;b_1j,t_2} + T_{jk;b_1j,b_2k} + (1-\delta_{k,n}\delta_{j,1})T_{jk;b_1j,b_2(k+1)} \\ & + T_{jk;b_1(j+1),t_2} + (1-\delta_{j+1,k})T_{jk;b_1(j+1),b_2k} + T_{jk;b_1(j+1),b_2(k+1)}\big) \\ & - (\delta_{j+1,k} + \delta_{k,n}\delta_{j,1})\,(T_{jk;2m1} + T_{jk;2m2}) - (T_{jk;B31} + T_{jk;B32})\end{aligned} \tag{4.39}$$

where we have inserted delta functions for special cases $k = (j+1)$ or $k = n, j = 1$.

Before ending this subsection, there is nice feature worth to mention about one-loop massless bubble singularities. It is well known that the integration of one-loop massless bubble is zero under proper regularization (such as dimensional regularization). We can also see it clearly at the integrand level in current setup. For one-loop massless bubble, the integrand is given by $\frac{N(\ell)}{\ell^2(\ell-p)^2}$. After the partial fraction and momentum shifting we get

$$\frac{N(\ell)}{\ell^2(-2\ell\cdot p)}+\frac{N(\ell)}{(\ell-p)^2(2\ell\cdot p)}\simeq\frac{N(\ell)}{\ell^2(-2\ell\cdot p)}+\frac{N(\ell+p)}{\ell^2(2\ell\cdot p)}\ . \tag{4.40}$$

Thus if $N(\ell)=N(\ell+P)$ (which is true for scalar theory), they cancel each other at the integrand level. It is worth to emphasize that the cancelation happens between two different orderings as having been observed in [41], i.e., the ordering $\{...,-\ell,\ell,p,...\}$ and the ordering $\{...,p,-\ell,\ell,...\}$. For two-loop massless bubble, we can do similar manipulation

$$\begin{aligned}
&\frac{N(\ell_1,\ell_2)}{\ell_1^2(\ell_1+p)^2(\ell_1-\ell_2+p)^2\ell_2^2(\ell_2-p)^2}\\
=&\ \frac{N(\ell_1,\ell_2)}{(\ell_1-\ell_2+p)^2}\left(\frac{1}{\ell_1^2(2\ell_1\cdot p)}+\frac{1}{(\ell_1+p)^2(-2\ell_1\cdot p)}\right)\left(\frac{1}{\ell_2^2(-2\ell_2\cdot p)}+\frac{1}{(\ell_2-p)^2(2\ell_2\cdot p)}\right)\\
\simeq&\ \frac{N(\ell_1,\ell_2)}{\ell_1^2\ell_2^2(\ell_1-\ell_2+p)^2(2\ell_1\cdot p)(-2\ell_2\cdot p)}+\frac{N(\ell_1,\ell_2+p)}{\ell_1^2\ell_2^2(\ell_1-\ell_2)^2(2\ell_1\cdot p)(2\ell_2\cdot p)}\\
&+\frac{N(\ell_1-p,\ell_2)}{\ell_1^2\ell_2^2(\ell_1-\ell_2)^2(-2\ell_1\cdot p)(-2\ell_2\cdot p)}+\frac{N(\ell_1-p,\ell_2+p)}{\ell_1^2\ell_2^2(\ell_1-\ell_2-p)^2(-2\ell_1\cdot p)(2\ell_2\cdot p)}\ .
\end{aligned}\tag{4.41}$$

Since the different mixed propagators $(\ell_1-\ell_2+p)^2$, $(\ell_1-\ell_2-p)^2$ and $(\ell_1-\ell_2+p)^2$, we see that even $N(\ell_1,\ell_2)=1$, they are not cancel each other at the integrand level. Because the explicit cancelation at the integrand level for one-loop massless bubble after summing over all orderings, we can save the explicit subtraction in (4.39) and simplify it to

$$\mathcal{I}^{CHY}_{\mathcal{O}_{jk}}=\{T_{jk}-(T_{jk;t_1}+T_{jk;t_2})+T_{jk;t_1,t_2}\}-(\delta_{j+1,k}+\delta_{k,n}\delta_{j,1})\,(T_{jk;2m1}+T_{jk;2m2})-(T_{jk;B31}+T_{jk;B32}) \tag{4.42}$$

One can sum up the first four terms to simplify to

$$T_{jk}\left(1-\frac{z_{j(-\ell_1)}z_{\ell_1(j+1)}}{z_{j\ell_1}z_{(-\ell_1)(j+1)}}\right)\left(1-\frac{z_{k(-\ell_2)}z_{\ell_2(k+1)}}{z_{k\ell_2}z_{(-\ell_2)(k+1)}}\right)=T_{jk}\frac{z_{j(j+1)}z_{(-\ell_1)\ell_1}}{z_{j\ell_1}z_{(-\ell_1)(j+1)}}\frac{z_{k(k+1)}z_{(-\ell_2)\ell_2}}{z_{k\ell_2}z_{(-\ell_2)(k+1)}}\ . \tag{4.43}$$

Although one can continue to add later four terms, (4.42) has more clear physical picture.

4.3.2 The CHY-integrand for ordering $\mathcal{O}_j$

Having done the ordering $\mathcal{O}_{jk}$, we consider the ordering $\mathcal{O}_j$. With this ordering, the full tree-level amplitude of $(n+4)$-legs is given by following CHY-integrand

$$T_j=\frac{1}{z_{12}^2...z_{j(-\ell_1)}^2z_{(-\ell_1)\ell_1}^2z_{\ell_1(-\ell_2)}^2z_{(-\ell_2)\ell_2}^2z_{\ell_2(j+1)}^2...z_{n1}^2} \tag{4.44}$$

Now we consider various forward limits, which can be produced in this ordering by checking the Figure 5, the Figure 6 and the Figure 7:

- First there are one-loop tadpole singularities, thus we have the corresponding CHY-integrands

$$T_{j;t_1}=T_j\mathcal{P}[j,-\ell_1,\ell_1,-\ell_2],\qquad T_{j;t_2}=T_j\mathcal{P}[\ell_1,-\ell_2,\ell_2,j+1] \tag{4.45}$$

  for ℓ_1-tadpoles and ℓ_2-tadpoles respectively.

- Secondly, there are one-loop massless bubbles. With j-th leg, there are bubbles with poles $s_{j(-\ell_1)}s_{j(-\ell_1)\ell_1}$ and its corresponding CHY-integrand is

$$T_{j;b_1 j} = T_j\mathcal{P}[j-1,j,-\ell_1,\ell_1]\mathcal{P}[j-1,j,\ell_1,-\ell_2] \ . \tag{4.46}$$

With $(j+1)$-th leg, there are bubbles with poles $s_{\ell_2(j+1)}s_{(-\ell_2)\ell_2(j+1)}$ and its corresponding CHY-integrand is

$$T_{j;b_2(j+1)} = T_j\mathcal{P}[-\ell_2,\ell_2,j+1,j+2]\mathcal{P}[\ell_1,-\ell_2,j+1,j+2] \ . \tag{4.47}$$

- Again, because the compatibility we have following four combinations between ℓ_1 one-loop forward singularities and ℓ_2 one-loop forward singularities:

$$T_{j;t_1,t_2} = T_j\mathcal{P}[j,-\ell_1,\ell_1,-\ell_2]\mathcal{P}[\ell_1,-\ell_2,\ell_2,j+1] \tag{4.48}$$

$$T_{j;t_1,b_2(j+1)} = T_j\mathcal{P}[j,-\ell_1,\ell_1,-\ell_2]\mathcal{P}[-\ell_2,\ell_2,j+1,j+2]\mathcal{P}[\ell_1,-\ell_2,j+1,j+2], \tag{4.49}$$

$$T_{j;b_1 j,t_2} = T_j\mathcal{P}[j-1,j,-\ell_1,\ell_1]\mathcal{P}[j-1,j,\ell_1,-\ell_2]\mathcal{P}[\ell_1,-\ell_2,\ell_2,j+1] \tag{4.50}$$

$$\begin{aligned} T_{j;b_1 j,b_2(j+1)} = {} & T_j\mathcal{P}[j-1,j,-\ell_1,\ell_1]\mathcal{P}[j-1,j,\ell_1,-\ell_2]\mathcal{P}[-\ell_2,\ell_2,j+1,j+2] \\ & \mathcal{P}[\ell_1,-\ell_2,j+1,j+2], \end{aligned} \tag{4.51}$$

- Now we discuss two-loop massless bubbles. Again let us start with two-loop bubble topologies. From Figure 6 we can see that beside the pole $s_{\ell_1(-\ell_2)}$, there is a free parameter k with $k=(j+1),(j+2),...,n,1,...,j-1$. For each k, there is one bubble structure with pole $s_{\ell_1(-\ell_2)}s_{(j+1)\dots k}s_{\ell_2(j+1)\dots k}s_{(k+1)\dots j}$ $s_{(k+1)\dots j(-\ell_1)}$ and the corresponding CHY-integrand is given by

$$\begin{aligned} T_{j;2m}[k] = {} & T_j\mathcal{P}[-\ell_1,\ell_1,-\ell_2,\ell_2]\mathcal{P}[\ell_2,j+1,k,k+1]\mathcal{P}[-\ell_2,\ell_2,k,k+1] \\ & \mathcal{P}[k,k+1,j,-\ell_1]\mathcal{P}[k,k+1,-\ell_1,\ell_1] \ . \end{aligned} \tag{4.52}$$

Again, for general k, they are massive bubbles. Only when $k=j+1$ or $k=j-1$ we get the massless bubbles. The CHY-integrands of both special cases can be trivially obtained from (4.52) by setting $k=j+1$ or $k=j-1$. For $k=j+1$, the factor $\mathcal{P}[\ell_2,j+1,k,k+1]=1$ while for $k=j-1$, the factor $\mathcal{P}[k,k+1,j,-\ell_1]=1$.

- The last piece we need to exclude is the (B-3) part in Figure 4. From Figure 7, we see that with the pole $s_{\ell_1(-\ell_2)}s_{\ell_2(j+1)\dots j}$, the CHY-integrand is given by

$$T_{j;B31} = T_j\mathcal{P}[-\ell_1,\ell_1,-\ell_2,\ell_2]\mathcal{P}[-\ell_2,\ell_2,j,-\ell_1] \ , \tag{4.53}$$

while with the pole $s_{\ell_1(-\ell_2)}s_{(j+1)\dots j(-\ell_1)}$, the CHY-integrand is given by

$$T_{j;B32} = T_j\mathcal{P}[-\ell_1,\ell_1,-\ell_2,\ell_2]\mathcal{P}[\ell_2,j+1,-\ell_1,\ell_1] \ . \tag{4.54}$$

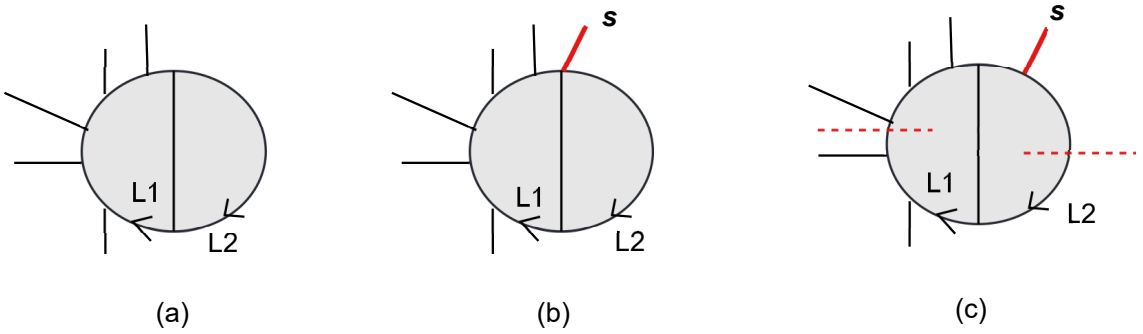

Figure 9: (a) The reducible two-loop diagrams; (b) After adding a particle at the vertex. However, this vertex has four legs. (c) Moving the added particle to ℓ_2-loop to make the vertex cubic. Furthermore, we have illustrated possible cuts for this cubic diagram.

Having above analysis, we can write down the CHY-integrand for the ordering $\mathcal{O}_j$ as

$$\begin{aligned}\mathcal{I}^{CHY}_{\mathcal{O}_j} = T_j - \left(T_{j;t_1} + T_{j;t_2} + T_{j;b_1 j} + T_{j;b_2(j+1)}\right) + \left(T_{j;t_1,t_2} + T_{j;t_1,b_2(j+1)} + T_{j;b_1 j,t_2} + T_{j;b_1 j,b_2(j+1)}\right)\\ -T_{j;2m}[j+1] - T_{j;2m}[j-1] - (T_{j;B31} + T_{j;B32})\end{aligned} \tag{4.55}$$

Again we can forget one-loop massless bubbles to simplify the expression, although we prefer the more complicated one (4.55).

4.4 The CHY-construction of reducible two-loop diagrams

As mentioned in the subsection 4.2, for two-loop diagrams, there are special two-loop diagrams (called the "reducible two-loop" diagrams), which will cause some troubles when we apply the partial fraction. After careful analysis, we have reduced the problem to the one-loop case in (4.12) and (4.13). Although as we have mentioned, we will treat this part as known data, tn this subsection, we will try to give a direct CHY-construction of these reducible two-loop diagrams at the two-loop level.

Let us recall the general expressions for reducible two-loop diagrams. From (a) of Figure 9 we can read out

$$\frac{1}{\ell_1^2(\prod_{i=1}^m(\ell_1+P_i))\ell_1^2(\ell_1-\ell_2)^2\ell_2^2} \tag{4.56}$$

under our choice of loop momenta. Now from these n external momenta k_i satisfying $\sum_{i=1}^n k_i = 0$, we try to construct $(n+1)$ massless momenta by following way. Picking up, for example, k_n and a massless momentum k_s such that $k_n \cdot k_s = 0$, then the $(n+1)$ massless momenta can be arranged to be $\{k_1, ..., k_{n-1}, k_n - tk_s, tk_s\}$. Using this construction, each diagram (a) in Figure 9 will have a corresponding diagram (b) in Figure 9 with the expression

$$\frac{1}{\ell_1^2(\prod_{i=1}^m(\ell_1+P_i)^2)(\ell_1-tk_s)^2(\ell_1-\ell_2)^2\ell_2^2} \tag{4.57}$$

It is easy to see that under the soft limit $t \to 0$, (4.57) reduces to (4.56). Although it looks nice, it is not the ϕ^3 theory since we have one vertex with four legs. We can remedy this by moving the leg s to the ℓ_2-loop as given by the diagram (c) in Figure 9. Thus (4.57) can be written as

$$(\ell_2 - tk_s)^2 \times \frac{1}{\ell_1^2(\prod_{i=1}^m(\ell_1+P_i)^2)(\ell_1-tk_s)^2(\ell_1-\ell_2)^2\ell_2^2(\ell_2-tk_s)^2} \tag{4.58}$$

Now formula (4.58) can have the CHY-construction by the standard procedure, i.e., partial fraction and momentum shifting, thus we arrive

$$\frac{-2t\widetilde{\ell}_2\cdot k_s}{\ell_1^2\ell_2^2}\mathcal{A}(\pm\widetilde{\ell}_1,\pm\widetilde{\ell}_2,1,...,k_n-tk_s,k_s) \tag{4.59}$$

where the $\mathcal{A}$ is certain tree-level amplitude with $(n+5)$-points, where $\widetilde{\ell}_1,\widetilde{\ell}_2$ are on-shell momenta in higher dimension.

Having above picture, now we can present the explicit CHY-construction for the term $\frac{1}{\ell_1^2(\ell_1-\ell_2)^2\ell_2^2}$ $\times\mathcal{I}^{1-loop}(1,2,...,n,\ell_1)$ in (4.13) as the soft limit $t\to 0$ of (4.59) (other terms in (4.13) can be obtained by cyclic permutations). The $\mathcal{A}$ is given by the sum over following orderings of trees:

$$\mathcal{O}_j = \{(-\ell_2,\ell_2),1,...,j,(-\ell_1,\ell_1),j+1,...,n,s\},\qquad j=0,1,...,n \tag{4.60}$$

where $j=0$ means the pair $(-\ell_1,\ell_1)$ is inserted before the leg 1. For the j-th ordering ($j\neq 0,n$), the signature of pole is $s_{s(-\ell_2)}s_{\ell_1(j+1)...n}s_{\ell_2 1...j(-\ell_1)}s_{1...j(-\ell_1)}$, thus the CHY-integrand is given by

$$T_j = \mathcal{I}_j\mathcal{P}[n,s,-\ell_2,\ell_2]\mathcal{P}[-\ell_1,\ell_1,n,s]\mathcal{P}[-\ell_2,\ell_2,-\ell_1,\ell_1]\mathcal{P}[\ell_2,1,-\ell_1,\ell_1] \tag{4.61}$$

with

$$\mathcal{I}_j = \frac{1}{z^2_{(-\ell_2)\ell_2}z^2_{\ell_2 1}...z^2_{j(-\ell_1)}z^2_{(-\ell_1)\ell_1}z^2_{\ell_1(j+1)}...z^2_{ns}z^2_{s(-\ell_2)}}\ . \tag{4.62}$$

For the $j=0$, the signature of pole is $s_{s(-\ell_2)}s_{\ell_1 1...n}s_{\ell_2(-\ell_1)}$, thus the CHY-integrand is given by

$$T_{j=0} = \mathcal{I}_{j=0}\mathcal{P}[n,s,-\ell_2,\ell_2]\mathcal{P}[-\ell_1,\ell_1,n,s]\mathcal{P}[-\ell_2,\ell_2,-\ell_1,\ell_1]\ . \tag{4.63}$$

For the $j=n$, the signature of pole is $s_{s(-\ell_2)}s_{\ell_1 s(-\ell_2)}s_{1...n(-\ell_1)}$, thus the CHY-integrand is given by

$$T_{j=n} = \mathcal{I}_{j=n}\mathcal{P}[\ell_1,s,-\ell_2,\ell_2]\mathcal{P}[-\ell_1,\ell_1,-\ell_2,\ell_2]\mathcal{P}[\ell_2,1,-\ell_1,\ell_1]\ . \tag{4.64}$$

Next we need to subtract forward singularities related to above orderings:

- The tadpole structure can appear when $j=0$ or $j=n$. For $j=0$ the signature will be $s_{s(-\ell_2)}s_{\ell_1 1...n}s_{\ell_2(-\ell_1)}$ multiplying by a further factor $s_{1...n}$, thus we have

$$T_{j=0;t} = T_{j=0}\mathcal{P}[\ell_1,1,n,s]\ . \tag{4.65}$$

  For $j=n$ the signature will be $s_{s(-\ell_2)}s_{\ell_1 s(-\ell_2)}s_{1...n(-\ell_1)}$ multiplying by a further factor $s_{1...n}$, thus we have

$$T_{j=n;t} = T_{j=n}\mathcal{P}[\ell_2,1,n,-\ell_1]\ . \tag{4.66}$$

- The massless bubble structure can appear when $j = 0, 1, n-1, n$. For $j = 0$ the signature will be $s_{s(-\ell_2)s_{\ell_1 1\ldots n}s_{\ell_2(-\ell_1)}}$ multiplying by either the factor $s_{\ell_1 1}s_{2..n}$ or $s_{1\ldots(n-1)}s_{\ell_1 1\ldots(n-1)}$, thus the corresponding CHY-integrands are

$$\begin{aligned} T_{j=0;b1} &= T_{j=0}\mathcal{P}[-\ell_1, \ell_1, 1, 2]\mathcal{P}[1, 2, n, s] \ , \\ T_{j=0;b2} &= T_{j=0}\mathcal{P}[-\ell_1, \ell_1, n-1, n]\mathcal{P}[\ell_1, 1, n-1, n] \ . \end{aligned} \tag{4.67}$$

  For $j = n$ the signature will be $s_{s(-\ell_2)s_{\ell_1 s(-\ell_2)}s_{1\ldots n(-\ell_1)}}$ multiplying by either the factor $s_{(-\ell_1)n}s_{1\ldots(n-1)}$ or $s_{2\ldots n}s_{2\ldots n(-\ell_1)}$, thus we have

$$\begin{aligned} T_{j=n;b1} &= T_{j=n}\mathcal{P}[n-1, n, -\ell_1, \ell_1]\mathcal{P}[\ell_2, 1, n-1, n] \ , \\ T_{j=n;b2} &= T_{j=n}\mathcal{P}[1, 2, n, -\ell_1]\mathcal{P}[1, 2, -\ell_1, \ell_1] \ . \end{aligned} \tag{4.68}$$

  For $j = 1$, the signature will be the one of $T_{j=1}$ multiplying by a further factor $s_{2\ldots n}$, thus the CHY-integrand is

$$T_{j=1;b} = T_{j=1}\mathcal{P}[\ell_1, 2, n, s] \ . \tag{4.69}$$

  For $j = n-1$, the signature will be the one of $T_{j=n-1}$ multiplying by a further factor $s_{1\ldots(n-1)}$, thus the CHY-integrand is

$$T_{j=n-1;b} = T_{j=n-1}\mathcal{P}[\ell_2, 1, n-1, -\ell_1] \ . \tag{4.70}$$

Putting all together, we finally arrive following CHY-integrand:

$$\mathcal{I}_{\mathcal{A}}(1, 2..., n) = \sum_{j=0}^{n} T_j - (T_{j=0;t} + T_{j=n;t}) - (T_{j=0;b1} + T_{j=0;b2} + T_{j=n;b1}T_{j=n;n2}) - (T_{j=1;b} + T_{j=n-1;b}) \tag{4.71}$$

Before ending this subsection, we want to remark that although we have provided a solution using the soft limit, more direct treatment is still preferred, but now we need to understand how to construct CHY-integrands with double poles at the tree-level. This will be an interesting thing to investigate.

5. Counting

Having reduced the two-loop problem to tree level (i.e., the loop scattering equations and the loop CHY-integrands) using the point of view of dimensional reduction, the checking of the proposal for two-loop becomes the checking of corresponding tree one. Since the later one has been extensively checked, both numerically and analytically (especially the powerful mapping rule), our proposal should be right. In this section, we will give a further evidence to support our claim by comparing the number of terms, produced by directly Feynman diagrams or by CHY-formula. In this section, contributions coming from reducible two-loop diagrams will be excluded.

5.1 Counting from CHY-formula

Since the whole result is obtained by summing over $2n$ orderings of $\mathcal{O}_j$ type and $n(n-1)$ orderings of $\mathcal{O}_{jk}$ type, we count terms from these two types one by one.

The $\mathcal{O}_j$ type: Let us start with the formula (4.55). The first term gives the full tree-level amplitude of $(n+4)$-points, so it gives $C(n+4)$ terms. For the $T_{j;t_1}$, since all tree diagrams have the pole $s_{(-\ell_1)\ell_2}$, these two legs have been effectively grouped to become one leg, thus all these diagrams become the tree-level diagrams of the $(n+3)$-points, so it gives $C(n+3)$ terms. For the $T_{j;B31}$ and $T_{j;B32}$, we see that they are effectively tree-level amplitudes of $(n+2)$-points. Similar arguments give

$$\begin{aligned}
\mathcal{N}[T_j] &= C(n+4), \quad \mathcal{N}[T_{j;t_1}] = \mathcal{N}[T_{j;t_2}] = C(n+3), \quad \mathcal{N}[T_{j;b_1 j}] = \mathcal{N}[T_{j;b_2(j+1)}] = C(n+2), \\
\mathcal{N}[T_{j;t_1,t_2}] &= C(n+2), \quad \mathcal{N}[T_{j;t_1,b_2(j+1)}] = \mathcal{N}[T_{j;b_1 j,t_2}] = C(n+1), \\
\mathcal{N}[T_{j;b_1 j,b_2(j+1)}] &= C(n), \quad \mathcal{N}[T_{j;B31}] = \mathcal{N}[T_{j;B32}] = C(n+2)
\end{aligned} \tag{5.1}$$

For general $T_{j;2m}[k]$, the counting is a little bit complicated. With a given k, we have two tree diagrams: one with $2+(k-j)$-legs and one with $n-(k-j)+2$-legs. Furthermore, external legs in each group will combine together before meeting ℓ_i (i.e., the tree-structure of $1+(k-j)$-points and $n-(k-j)+1$-points), thus we will have the counting $C(k-j+1)C(n-(k-j)+1)$. However, for massless bubbles, we just need to consider the case $k-j=1$ or $n-(k-j)=1$ and both cases give $C(n)$ terms.

Putting all together, we finally arrive

$$\mathcal{N}[\mathcal{O}_j] = C(n+4) - 2C(n+3) - 3C(n+2) + 2C(n+1) - C(n) \ . \tag{5.2}$$

This expression does not depend on the value of j as it should. There are $2n$ of this type, so the final number of terms coming from this type should be

$$\mathcal{N}_I = 2n\left\{C(n+4) - 2C(n+3) - 3C(n+2) + 2C(n+1) - C(n)\right\} \ . \tag{5.3}$$

The $\mathcal{O}_{jk}$ type: For this one, we start with (4.39) with $1 \le j < k \le n$. Using similar arguments we give the counting for each piece:

$$\begin{aligned}
\mathcal{N}[T_{jk}] &= C(n+4), \quad \mathcal{N}[T_{jk;t_1}] = \mathcal{N}[T_{jk;t_2}] = C(n+3), \quad \mathcal{N}[T_{jk;t_1,t_2}] = C(n+2), \\
\mathcal{N}[T_{jk;b_1 j}] &= \mathcal{N}[T_{jk;b_1(j+1)}] = \mathcal{N}[T_{jk;b_2 k}] = \mathcal{N}[T_{jk;b_2(k+1)}] = C(n+2), \\
\mathcal{N}[T_{jk;t_1,b_2 k}] &= \mathcal{N}[T_{jk;t_1,b_2(k+1)}] = \mathcal{N}[T_{jk;b_1(j+1),t_2}] = \mathcal{N}[T_{jk;b_1 j,b_2 k}] = C(n+1), \\
\mathcal{N}[T_{jk;b_1 j,b_2 k}] &= \mathcal{N}[T_{jk;b_1(j+1),b_2(k+1)}] = \mathcal{N}[T_{jk;b_1(j+1),b_2 k}] = \mathcal{N}[T_{jk;b_1(j+1),b_2(k+1)}] = C(n), \\
\mathcal{N}[T_{jk;2m1}] &= \mathcal{N}[T_{jk;2m2}] = C(k-j+1)C(n-(k-j)+1), \\
\mathcal{N}[T_{jk;B31}] &= \mathcal{N}[T_{jk;B32}] = C(k-j+2)C(n-(k-j)+2) \ .
\end{aligned} \tag{5.4}$$

Thus from (4.39) we get

$$\mathcal{N}[\mathcal{Q}_{jk}] = C(n+4) - 2C(n+3) - 3C(n+2) + 4C(n+1) + (4 - \delta_{j+1,k} - \delta_{k,n}\delta_{j,1})C(n)$$
$$-2(\delta_{j+1,k} + \delta_{k,n}\delta_{j,1})C(k-j+1)C(n-(k-j)+1) - 2C(k-j+2)C(n-(k-j)+2)\ . \quad (5.5)$$

Thus when $k = j+1$ or $k = n, j = 1$, the counting is given by

$$\mathcal{N}^s = C(n+4) - 2C(n+3) - 3C(n+2) + 4C(n+1) + 3C(n) - 2C(n) - 2C(n+1)$$
$$= C(n+4) - 2C(n+3) - 3C(n+2) + 2C(n+1) + C(n)\ . \quad (5.6)$$

For other cases, we have

$$\mathcal{N}^g[\mathcal{Q}_{jk}] = C(n+4) - 2C(n+3) - 3C(n+2) + 4C(n+1) + 4C(n)$$
$$-2C(k-j+2)C(n-(k-j)+2)\ . \quad (5.7)$$

Now we sum up all pairs of (j,k). For special cases, there are $2n$ of them, so we have

$$\mathcal{N}_{II,A} = 2n\mathcal{N}^s = 2n\left\{C(n+4) - 2C(n+3) - 3C(n+2) + 2C(n+1) + C(n)\right\}. \quad (5.8)$$

For other cases with number $n(n-1) - 2n$, we have the sum

$$\mathcal{N}_{II,B} = 2\left\{\sum_{k=3}^{n-1}\mathcal{N}^g[\mathcal{Q}_{j=1,k}] + \sum_{j=2}^{n-2}\sum_{k=j+2}^{n}\mathcal{N}^g[\mathcal{Q}_{jk}]\right\}. \quad (5.9)$$

Summary: The total number of terms given by the CHY-formula is

$$\mathcal{N}_{CHY} = \mathcal{N}_I + \mathcal{N}_{II,A} + \mathcal{N}_{II,B}\ . \quad (5.10)$$

5.2 Counting from Feynman diagrams

Now we do the counting using Feynman diagrams given in Figure 4 directly. Although we will count terms for Type (A) and Type (B) separately, they do share same one-loop building block as indicated by the red square in Figure 4 (the n_L part of Type A), thus we need to consider terms contributing from the building block first. To deal with it, it is crucial to recall that after applying the partial fraction to expression $\frac{1}{\prod(\ell+K_i)^2}$, we will get terms like $\frac{1}{(\ell_1+K_i)^2} \times F_i$ for each K_i. Now we count terms with the same propagator $\frac{1}{(\ell_1+K_i)^2}$. Since the partial fraction has the physical picture as cutting this propagator and putting it on-shell, the building block has been separated to two trees. One has n_1 external legs at the lower part (so the whole structure is the tree of (n_1+2)-points), while another one has $n_2 = n_L - n_1$ external legs at the upper part (so the whole structure is the tree of (n_2+2)-points). Using the formula (2.5) we get the number of terms related to this propagator is $C(n_1+2)C(n-n_1+2)$. Summing over all splitting, we get the number of terms for the one-loop building block to be

$$\mathcal{B}(n) = \sum_{n_1=0}^{n} C(n_1+2)C(n-n_1+2). \quad (5.11)$$

Having the building block, we can count terms for these two types of diagrams in Figure 4. For the Type (A), since we ask $n_L, n_R \geq 2$ to avoid one-loop tadpoles and one-loop massless bubbles, the total number of terms is given by

$$\mathcal{N}_{F;A}(n) = n \sum_{n_L=2}^{n-2} \sum_{n_R=2}^{n-n_L} \mathcal{B}(n_L)\mathcal{B}(n_R)C(n-n_L-n_R+2)(n-n_L-n_R+1) \ . \tag{5.12}$$

Let us give a brief explanation of formula (5.12). First the factor n comes from the sum over all cyclic orderings. The cyclic sum makes also the two loop momenta ℓ_1, ℓ_2 symmetric in the integrand. Secondly, the sum is over all possible distributions of n legs into four subsets n_L, m_u, m_d, n_R with constraints that $n_L \geq 2, n_R \geq 2$ and $m_u, m_d \geq 0$. Thirdly, from the Feynman diagrams, it can be seen that the middle part is just the tree-level amplitude of $(2+m_u+m_d) = (n-n_L-n_R+2)$-points. Furthermore, there are $(n-n_L-n_R+1)$ ways to distribute to m_u, m_d given n_L, n_R, so the contribution from the middle part is given by $C(n-n_L-n_R+2)(n-n_L-n_R+1)$.

For the Type (B), the counting is much simpler. Using the formula for our building block, we get

$$\mathcal{N}_{F;B}(n) = n \sum_{n_L=1}^{n-1} \mathcal{B}(n_L)\mathcal{B}(n-n_L) - 2^3 n C(n) \tag{5.13}$$

Now let us explain formula (5.13). First the factor n comes again from the sum over the cyclic orderings. Secondly, to exclude reducible two-loop diagrams, we require $n_L \geq 1, n_R \geq 1$ when we sum over all different distributions of n to n_L and n_R. Furthermore, There are two special cases corresponding to two-loop massless bubbles. One is $n_L = 1$ and another one, $n_R = 1$. They are multiplying by $C(n)$ because the remaining $(n-1)$-legs must be grouped together to become one. The factor 2^3 is because each massless bubble will produce four trees by different combinations of two cuts, while another two comes from two choices of either $n_L = 1$ or $n_R = 1$.

Summing these two parts together, finally we get the number of terms after the partial fraction using expressions from Feynman diagrams

$$\mathcal{N}_F(n) = \mathcal{N}_{F;B}(n) + \mathcal{N}_{F;A}(n) \tag{5.14}$$

Comparison: It can be checked that (5.14) is equal to (5.10) although they are completely different expressions. The matching serves as a strong consistent check.

6. Conclusion

In this paper, we have established the all-loop scattering equations by deforming the loop momenta to higher dimension. Under this new aspect, we have effectively reduced the loop problem to the forward limit of corresponding tree one. One technical difficulty of this construction is to remove forward singularities of

corresponding tree parts. Using the bi-adjoint ϕ^3 theory, we have demonstrated how to achieve this goal for two-loop planar integrands. The method is based on a nice understanding of the mapping rule, especially how to construct the CHY-integrand which produces tree amplitudes with a fixed pole structure. We have supported our two-loop results of ϕ^3 theory by matching the number of terms obtained using two different methods.

Although we have focused on the planar part only in this paper, we think the same idea should work for non-planar part as well as not color ordered loop amplitudes. We believe that our construction should be able to generalize to higher loops, at least for ϕ^3 theory. Another important thing is to understand how to remove the forward singularities of Yang-Mills and Gravity theories based on our results.

Acknowledgments

We would like to thank the early participant of Christian Baadsgaard, N. E. J. Bjerrum-Bohr, Jacob L. Bourjaily, Simon Caron-Huot and Poul H. Damgaard. We would also like to thank discussions with Song He, Rijun Huang, Qinjun jin, Minxin Luo, Junjie Rao and suggestions for draft by N. E. J. Bjerrum-Bohr, Poul H. Damgaard and Rijun Huang. Last but not least we would like to thank the hospitality of the Niels Bohr International Academy where this project was initiated. This work is supported by the Qiu-Shi Fund and the Chinese NSF under contracts No.11135006, No.11125523 and No.11575156.

References

[1] F. Cachazo, S. He, and E. Y. Yuan, "Scattering Equations and Kawai-Lewellen-Tye Orthogonality," *Phys. Rev.* **D90** (2014) no. 6, 065001, arXiv:1306.6575 [hep-th].

[2] F. Cachazo, S. He, and E. Y. Yuan, "Scattering of Massless Particles in Arbitrary Dimensions," *Phys. Rev. Lett.* **113** (2014) no. 17, 171601, arXiv:1307.2199 [hep-th].

[3] F. Cachazo, S. He, and E. Y. Yuan, "Scattering of Massless Particles: Scalars, Gluons and Gravitons," *JHEP* **1407** (2014) 033, arXiv:1309.0885 [hep-th].

[4] F. Cachazo, S. He and E. Y. Yuan, "Einstein-Yang-Mills Scattering Amplitudes From Scattering Equations," JHEP **1501**, 121 (2015) [arXiv:1409.8256 [hep-th]].

[5] F. Cachazo, S. He and E. Y. Yuan, "Scattering Equations and Matrices: From Einstein To Yang-Mills, DBI and NLSM," JHEP **1507**, 149 (2015) doi:10.1007/JHEP07(2015)149 [arXiv:1412.3479 [hep-th]].

[6] Fairlie, David and Roberts, David, "Dual Models without Tachyons - a New Approach", unpublished Durham preprint PRINT-72-2440, 1972.

[7] Roberts, David, "Mathematical Structure of Dual Amplitudes", Durham University, 1972, Available at Durham E-Theses online.

[8] Fairlie, David B., "A Coding of Real Null Four-Momenta into World-Sheet Co-ordinates", Adv. Math. Phys., 2009,284689, DOI="10.1155/2009/284689", arXiv:0805.2263.

[9] Gross, David J. and Mende, Paul F., "String Theory Beyond the Planck Scale", Nucl. Phys.B303,1988,407, DOI="10.1016/0550-3213(88)90390-2".

[10] Witten, Edward, "Parity invariance for strings in twistor space", Adv. Theor. Math. Phys.8,2004,779-796, DOI="10.4310/ATMP.2004.v8.n5.a1", arXiv:hep-th/0403199.

[11] Caputa, Pawel and Hirano, Shinji, "Observations on Open and Closed String Scattering Amplitudes at High Energies", JHEP02(2012)111, DOI="10.1007/JHEP02(2012)111", arXiv:1108.2381

[12] Caputa, Pawel, "Lightlike contours with fermions", Phys. Lett.B716, 2012,475-480. DOI="10.1016/j.physletb.2012.09.006", arXiv:1205.6369.

[13] Makeenko, Y. and Olesen, "The QCD scattering amplitude from area behaved Wilson loops", Phys. Lett.B709,2012,285-288, DOI= "10.1016/j.physletb.2012.02.032", arXiv:1111.5606.

[14] Cachazo, Freddy, "Fundamental BCJ Relation in N=4 SYM From The Connected Formulation". ARXIV:1206.5970;

[15] L. Dolan and P. Goddard, "Proof of the Formula of Cachazo, He and Yuan for Yang-Mills Tree Amplitudes in Arbitrary Dimension," *JHEP* **1405** (2014) 010, arXiv:1311.5200 [hep-th].

[16] R. Britto, F. Cachazo and B. Feng, "New recursion relations for tree amplitudes of gluons," Nucl. Phys. B **715**, 499 (2005) [hep-th/0412308].

[17] R. Britto, F. Cachazo, B. Feng and E. Witten, "Direct proof of tree-level recursion relation in Yang-Mills theory," Phys. Rev. Lett. **94**, 181602 (2005) [hep-th/0501052].

[18] L. Mason and D. Skinner, "Ambitwistor Strings and the Scattering Equations," *JHEP* **1407** (2014) 048, arXiv:1311.2564 [hep-th].

[19] N. Berkovits, "Infinite Tension Limit of the Pure Spinor Superstring," *JHEP* **1403** (2014) 017, arXiv:1311.4156 [hep-th].

[20] H. Gomez and E. Y. Yuan, "N-Point Tree-Level Scattering Amplitude in the New Berkovits' String," *JHEP* **1404** (2014) 046, arXiv:1312.5485 [hep-th].

[21] T. Adamo, E. Casali, and D. Skinner, "Ambitwistor Strings and the Scattering Equations at One Loop," *JHEP* **1404** (2014) 104, arXiv:1312.3828 [hep-th].

[22] Y. Geyer, A. E. Lipstein and L. J. Mason, "Ambitwistor Strings in Four Dimensions," Phys. Rev. Lett. **113**, no. 8, 081602 (2014) [arXiv:1404.6219 [hep-th]].

[23] Y. Geyer, A. E. Lipstein and L. Mason, "Ambitwistor strings at null infinity and (subleading) soft limits," Class. Quant. Grav. **32**, no. 5, 055003 (2015) [arXiv:1406.1462 [hep-th]].

[24] E. Casali and P. Tourkine, "Infrared Behaviour of the One-Loop Scattering Equations and Supergravity Integrands," *JHEP* **04** (2015) 013, arXiv:1412.3787 [hep-th].

[25] T. Adamo and E. Casali, "Scattering equations, supergravity integrands, and pure spinors," JHEP **1505**, 120 (2015) [arXiv:1502.06826 [hep-th]].

[26] K. Ohmori, "Worldsheet Geometries of Ambitwistor String," JHEP **1506**, 075 (2015) [arXiv:1504.02675 [hep-th]].

[27] E. Casali, Y. Geyer, L. Mason, R. Monteiro and K. A. Roehrig, "New Ambitwistor String Theories," arXiv:1506.08771 [hep-th].

[28] Y. Geyer, L. Mason, R. Monteiro and P. Tourkine, "Loop Integrands for Scattering Amplitudes from the Riemann Sphere," Phys. Rev. Lett. **115**, no. 12, 121603 (2015) doi:10.1103/PhysRevLett.115.121603 [arXiv:1507.00321 [hep-th]].

[29] N. E. J. Bjerrum-Bohr, P. H. Damgaard, P. Tourkine, and P. Vanhove, "Scattering Equations and String Theory Amplitudes," *Phys. Rev.* **D90** (2014) no. 10, 106002, arXiv:1403.4553 [hep-th].

[30] C. Baadsgaard, N. E. J. Bjerrum-Bohr, J. L. Bourjaily and P. H. Damgaard, "Integration Rules for Scattering Equations," JHEP **1509**, 129 (2015) doi:10.1007/JHEP09(2015)129 [arXiv:1506.06137 [hep-th]].

[31] C. Baadsgaard, N. E. J. Bjerrum-Bohr, J. L. Bourjaily and P. H. Damgaard, "Scattering Equations and Feynman Diagrams," JHEP **1509**, 136 (2015) doi:10.1007/JHEP09(2015)136 [arXiv:1507.00997 [hep-th]].

[32] C. Baadsgaard, N. E. J. Bjerrum-Bohr, J. L. Bourjaily, P. H. Damgaard and B. Feng, "Integration Rules for Loop Scattering Equations," JHEP **1511**, 080 (2015) doi:10.1007/JHEP11(2015)080 [arXiv:1508.03627 [hep-th]].

[33] L. Dolan and P. Goddard, "The Polynomial Form of the Scattering Equations," JHEP **1407**, 029 (2014) [arXiv:1402.7374 [hep-th]].

[34] C. Kalousios, "Scattering equations, generating functions and all massless five point tree amplitudes," JHEP **1505**, 054 (2015) [arXiv:1502.07711 [hep-th]].

[35] R. Huang, J. Rao, B. Feng and Y. H. He, "An Algebraic Approach to the Scattering Equations," JHEP **1512**, 056 (2015) doi:10.1007/JHEP12(2015)056 [arXiv:1509.04483 [hep-th]].

[36] M. Sogaard and Y. Zhang, "Scattering Equations and Global Duality of Residues," arXiv:1509.08897 [hep-th].

[37] L. Dolan and P. Goddard, "General Solution of the Scattering Equations," arXiv:1511.09441 [hep-th].

[38] C. Cardona and C. Kalousios, "Elimination and recursions in the scattering equations," arXiv:1511.05915 [hep-th].

[39] C. Cardona and C. Kalousios, "Comments on the evaluation of massless scattering," arXiv:1509.08908 [hep-th].

[40] F. Cachazo and H. Gomez, "Computation of Contour Integrals on $\mathcal{M}_{0,n}$," arXiv:1505.03571 [hep-th].

[41] C. Baadsgaard, N. E. J. Bjerrum-Bohr, J. L. Bourjaily, P. H. Damgaard and B. Feng, "Integration Rules for Loop Scattering Equations," arXiv:1508.03627 [hep-th].

[42] S. He and E. Y. Yuan, "One-loop Scattering Equations and Amplitudes from Forward Limit," Phys. Rev. D **92**, no. 10, 105004 (2015) doi:10.1103/PhysRevD.92.105004 [arXiv:1508.06027 [hep-th]].

[43] Y. Geyer, L. Mason, R. Monteiro and P. Tourkine, "One-loop amplitudes on the Riemann sphere," arXiv:1511.06315 [hep-th].

[44] F. Cachazo, S. He and E. Y. Yuan, "One-Loop Corrections from Higher Dimensional Tree Amplitudes," arXiv:1512.05001 [hep-th].

[45] C. Baadsgaard, N. E. J. Bjerrum-Bohr, J. L. Bourjaily, S. Caron-Huot, P. H. Damgaard and B. Feng, "New Representations of the Perturbative S-Matrix," arXiv:1509.02169 [hep-th].

[46] R. Huang, Q. Jin, J. Rao, K. Zhou and B. Feng, "The $\mathcal{Q}$-cut Representation of One-loop Integrands and Unitarity Cut Method," arXiv:1512.02860 [hep-th].

[47] S. G. Naculich, "Scattering equations and BCJ relations for gauge and gravitational amplitudes with massive scalar particles," JHEP **1409**, 029 (2014) doi:10.1007/JHEP09(2014)029 [arXiv:1407.7836 [hep-th]].

[48] S. G. Naculich, "CHY representations for gauge theory and gravity amplitudes with up to three massive particles," JHEP **1505**, 050 (2015) doi:10.1007/JHEP05(2015)050 [arXiv:1501.03500 [hep-th]].

[49] S. G. Naculich, "Amplitudes for massive vector and scalar bosons in spontaneously-broken gauge theory from the CHY representation," JHEP **1509**, 122 (2015) doi:10.1007/JHEP09(2015)122 [arXiv:1506.06134 [hep-th]].

[50] C. S. Lam and Y. P. Yao, "Off-Shell CHY Amplitudes," arXiv:1511.05050 [hep-th].

[51] S. Caron-Huot, "Loops and trees," JHEP **1105**, 080 (2011) doi:10.1007/JHEP05(2011)080 [arXiv:1007.3224 [hep-ph]].